Is there a Future for Event Display?

H.Drevermann, CERN, Geneva
D.Kuhn, Institut für Experimentalphysik der Universität Innsbruck[1]
B.S.Nilsson, CERN, Geneva, and Niels Bohr Institute, Copenhagen

1. Introduction

High energy physics experiments investigate reactions between colliding elementary particles. To this purpose data on the particles leaving the collision point are recorded in large detectors and stored in digital form. The set of data recorded per collision is called an event. Practically all subdetectors are sampling devices, which for each event record the tracks of charged particles as a sequence of points, called hits, or record the showers of particles as a set of cells, for which the energy deposited is recorded as well. The events are the basic units for further investigations, which are done by powerful pattern recognition and analysis programs. For checking of these methods and for presentation, the display of single events is an efficient tool, as visual representation is the most efficient way to transfer data from a computer to the human brain.

However, complexity of both events and detectors has increased substantially and will increase further. Higher event multiplicities and higher momenta of outgoing particles can be matched by more sophisticated detectors, i.e. detectors with a growing number of subunits of increasing granularity, resolution and precision. As a consequence pictures of detectors and events are getting more and more complicated and, in the extreme, may even get incomprehensible, conveying the only message, that the experiment is complicated. The enormous improvements of detectors, of computers and of visual devices seem not to be matched by the "perception techniques" of the human eye and the human brain, as these have been developed a long time ago for other objects than pictures of events. This leads to the question: Is a fast, efficient and unambiguous transfer of data to the human brain via visual techniques still possible or will it be more convenient to read and interpret numbers?

To answer this question, it is necessary to study conventional representations and possible improvements. However, it will turn out for a variety of applications, that conventional representations result in pictures, which are not sufficiently clear. Therefore new visual representations are proposed here, which can better be tuned to the capabilities of human perception.

For the use of graphical representations in talks and papers it is necessary to find pictures, which can be understood intuitively without omitting relevant information. For this purpose we will discuss:

- the selection of clear views,
- methods to present histograms,
- coloring schemes.

For the checking of detector performance and programming tools for the extraction of the relevant information, one needs independent methods. One of the best methods to fulfill this task

1. Supported by grant of Fonds zur Förderung der Wissenschaftlichen Forschung, Austria

is visual analysis, which normally can be applied only to a small subsample of the large amount of events recorded in a typical experiment. Visual analysis may even go beyond the capabilities of existing methods in recognizing specific event features. It will be shown here, that there are ways of visual data presentation beyond the conventional 2D and 3D techniques, which facilitate these tasks considerably. We will discuss in detail:

- the selection of special representations,
- methods of picture transformation in two and three dimensions,
- the association of tracking information to data of scalar fields (e.g. Lego plot),
- representation of scalar fields in two and three dimensions.

Most of the techniques discussed here were applied and developed for the ALEPH experiment at LEP/CERN [1]. Their direct application to other experimental setups is restricted to cylindrical detectors with a homogeneous solenoidal field. However, it seems possible to modify these techniques to be applied to different setups. In some cases this will be done here through a generalization of the methods and subsequent application to other experimental devices, namely to tracking detectors outside a magnetic field or experiments without magnetic field.

These techniques are incorporated in the graphics program DALI which runs on simple workstations.

2. Pictures for Talks and Papers

Pictures of events are often used in talks and papers to underline and clarify, what is said, i.e. to show, what would be lengthy and difficult to explain in words. Such pictures must be easily and intuitively understood, requiring normally only short explanations. The listener or reader should be allowed to assume that his intuitive understanding of the picture is right, for example that objects which seem to be connected are connected. It is the speaker's or writer's responsibility to guarantee, that the impression one gets from a picture is the right one.

2.1. Front and Side View

If no event is shown, a detector is best displayed in a technique called cut away perspective view. This resembles a photo of the real detector, where parts of it are cut away to show its interior. For the simultaneous representation of the detector and an event, however, this technique is normally not applicable. In this case the detector is drawn usually in what is called the wire frame technique. Figures 1a and d show perspective projections in this technique.

These pictures, however, are too crowded with lines and need to be simplified. This is done in the *Y* versus *X* projection (*Y/X: Y*=ordinate, *X*=abscissa) in figure 1b and in *Y/Z* in figure 1e. The *Z*-axis is equal to the cylinder axis, i.e. the beam axis. Compared to the perspective projections, the number of visible lines in *Y/X* and *Y/Z* is typically reduced by a factor three.

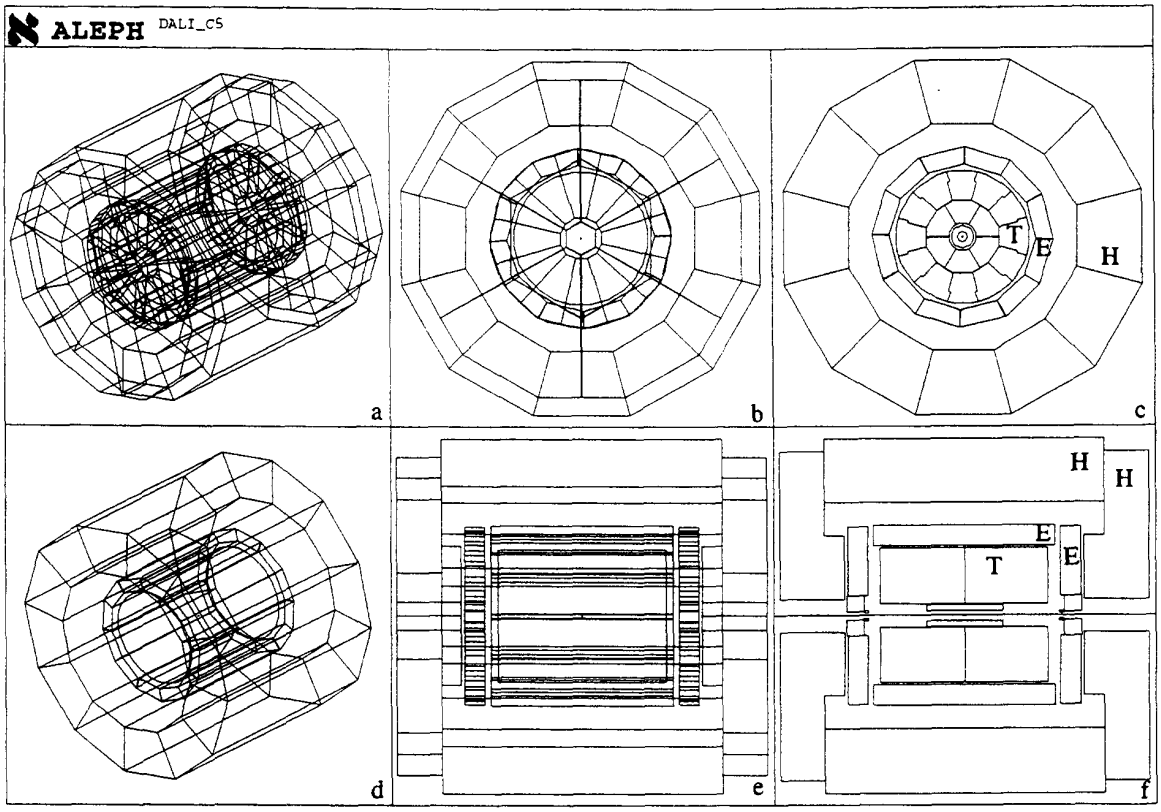

Fig. 1: Drawing of the barrel and endcaps of the HCAL(H), ECAL(E) and TPC(T) in the projections:
a) perspective b) Y/X c) Y/X without endcaps, with TPC sectors
d) perspective without endcaps e) Y/Z f) ρ'/Z with inner detectors

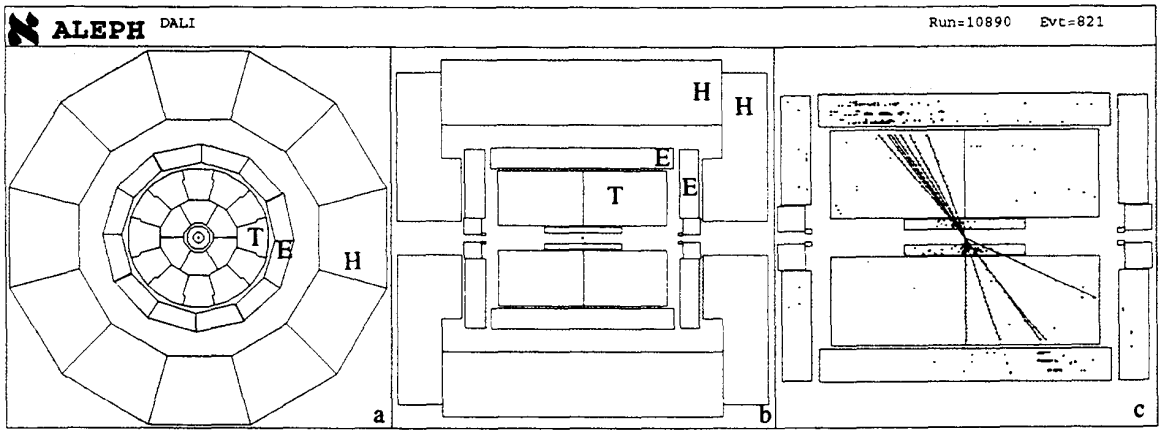

Fig. 2: Setting the background to grey
a) Y/X b) ρ'/Z c) ρ'/Z of ECAL and TPC with hits and tracks

These projections, however, suffer still from the fact, that different subdetectors are superimposed onto each other[1]. This problem can be solved, if the projections *Y/X* and *Y/Z* are replaced by pictures of cross-sections through the detector center perpendicular (fig 1c) or parallel (fig 1f) to the *Z*-axis.

1. In *Y/X* the ECAL and HCAL endcaps and the TPC overlap, in *Y/Z* the ECAL,HCAL barrel and the TPC.

However, in such cross-sections events cannot be displayed in a useful way, since a cross-section through a line yields normally only one point. Therefore, one needs projections, which on one side preserve the line character of tracks and on the other side result in the same detector images as the ones obtained from cross-sections.

In the case of the ALEPH detector and of similar ones with cylindrical structure, the *Y/X* projection with endcaps omitted is identical to the cross-section perpendicular to the cylinder axis (front view). This type of picture will be called *Y/X* from now on.

The cross-section parallel to the cylinder axis (side view) is identical to a ρ'/Z projection, where ρ' is defined as $\rho' = \pm\rho = \pm\sqrt{X^2 + Y^2}$ with the sign depending on the azimuthal angle ($\varphi = \text{atan}\frac{Y}{X}$) of the object to be drawn; $\rho' = +\rho$, if $\varphi_1 < \varphi < \varphi_1 + 180°$ and $\rho' = -\rho$, otherwise, where φ_1 is interactively defined. In ρ'/Z the event is cut into two unconnected halves (see figure 2c) and even single tracks may be cut into two pieces.

If in the case of *Y/X* as defined above, hits in the omitted endcaps are not drawn[1]. For both projections, *Y/X* and ρ'/Z, the following rules hold in this case for the observer:

- hits lie inside the subdetector, from which they originate, so that their source is obvious. That means also, that
- hits or tracks are visible only if the corresponding subdetector is drawn,.

These features, which facilitate interpretation considerably, are lacking in the other projections of figure 1.

The detector elements show up more clearly, if the background around and between them is shaded or colored (compare figures 2a,b to the figures 1c and f and see color plate 1). The coloring of the subdetector areas is improved considerably by overlaying the wireframe, which facilitates the understanding of the structure of the subdetectors. There is a clear improvement as compared to the mere wireframe picture, especially if a detector section is shown (see color plate 1 d,e,f).

2.2. The Fish Eye Transformation of Y/X.

In the case of radial symmetric pictures, as the *Y/X* projection of a cylindrical or quasi cylindrical detector such as ALEPH, the scale may be decreased with increasing radius, so that the outer detectors are shrunk. For a constant total picture size the inner subdetectors are hence enlarged (compare figure 3a and c). This emphasizes the commonly used construction principle of detectors, namely that precision and sampling distance decrease, when stepping from the inner to the outer detectors (see color plate 3).

This so called fish eye transformation is calculated in the following way: From the cartesian coordinates X and Y the spherical coordinates ρ and φ are derived. These are transformed to ρ_F and φ_F by: $\rho_F = \frac{\rho}{1 + a\rho}$ and $\varphi_F = \varphi$.

From ρ_F and φ_F the cartesian coordinates X_F and Y_F are recalculated and drawn with a suitable linear scale to conserve the total picture size. The factor a is chosen interactively [2].

---

1. For the display of tracks going into an endcap, ρ'/Z is the only good, intuitively understandable projection.

The non linear fish eye transformation gets linear for small ρ ($a\rho \ll 1 \Rightarrow \rho \approx \rho_F$) avoiding a singularity at the origin (compare the inner region of the fish eye view to the linearly scaled picture of the inner detectors in figure 3 b).

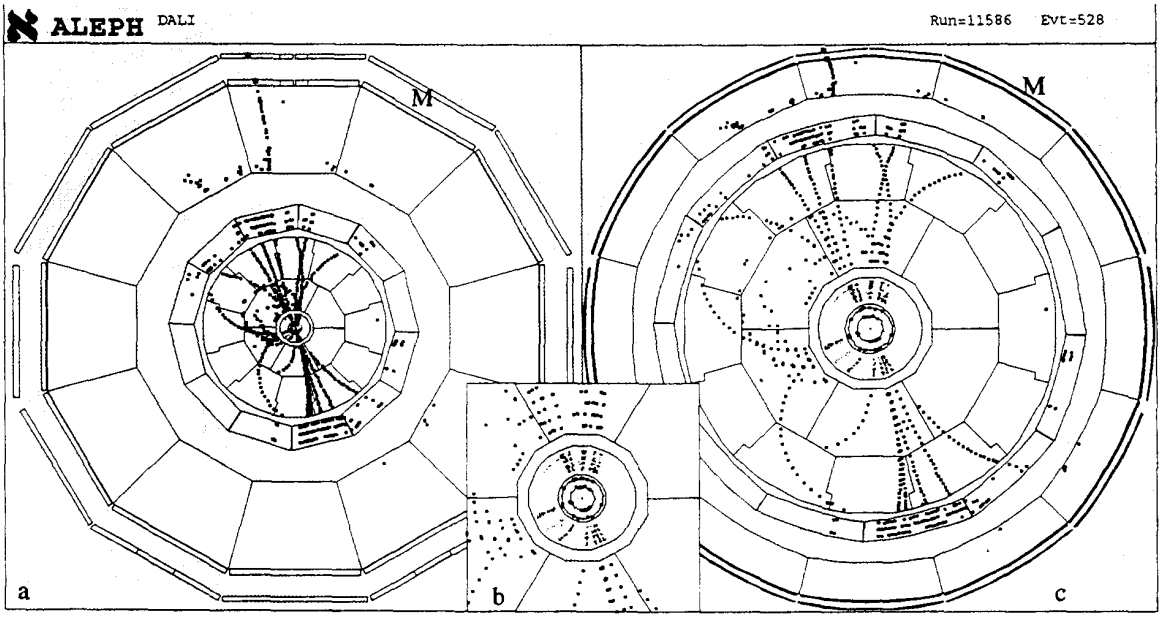

Fig. 3: Y/X projection from the center up to the Muon Detector (M) with an event
a) linear scale b) linear blow-up of the centre c) fish eye view

The application of this technique to non radial pictures, e.g. to ρ'/Z, yields pictures of rather difficult interpretation [1].

2.3. Histograms in a Picture

Particles showering in calorimeters or just traversing them deposit energy. In order to represent the position of the cells and the deposited energy, the active cells of size $\Delta_1,\Delta_2,\Delta_3$ and their energy deposit E are commonly displayed by representing them as boxes of size Δ_1,Δ_2, kE, i.e. the length of one side is replaced by the properly scaled energy E.

If a projection is chosen, in which the cells line up behind each other, one gets a picture as seen in color plate 2a which resembles a "wire frame skyline". This representation differs from a histogram, where the energies of cells lining up behind each other are added. Different modes of presenting such histograms are shown in color plate 2b - 2f as wire frame (2b), structured wire frame (2c), unframed area (2d), framed area (2e) and structured area (2f). Experience shows, that histograms drawn as structured areas (2f) are preferred by the users. If drawn as wireframe only, the structuring yields a more complicated picture (2c) compared to the unstructured wireframe (2b).

If histograms are displayed in a picture of radial structure they are best drawn as radial histograms (see Color plates 2 - 4). Even so the detector image is rectangular in ρ'/Z, radial histograms underline better the radial event structure (see color plates 4 and 5).

It may occur, that histograms from different detectors overlay each other. In order not

1. Examples of such pictures are found in the numerous works of the painter M.C.Escher.

to loose relevant information, four methods may be applied:

- Scaling down of the histograms, in order to avoid overlapping.
- Drawing both histograms as wire frames (see color plate 4a).
- Drawing the first histogram as structured area and the second one on top but as wire frame only.
- Drawing both histograms as structured areas, but in the following sequence: histogram 1, then histogram 2, then the wire frame of both histograms (see color plate 4b, histogram 1 = white, 2 = yellow).

Experience shows, that the last method produces the clearest pictures, but necessitates two passes to draw the same data.

2.4. Application of Colors

The choice of colors depends primarily on the size of the objects to be drawn and on the background, which they are drawn onto. The width of hits and tracks, i.e. points and lines, should be kept sufficiently small, in order to resolve them properly. However, in the case of small objects the human eye distinguishes only very few colors. In other words, it is the number of requested colors, which defines the object size. A good compromise is the use of the following colors: white or black, green, yellow, orange, red, magenta, blue, cyan and grey (see color plate 6a).

This reduced set of colors is in most cases not sufficient to convey any geometrical information (e.g. the depth of an object), i.e. it cannot be used as representation of a third dimension. Colors are however very useful to associate objects on different pictures side by side (see in color plates 5 and compare to color plate 5). This method can even be extended to lists, thus combining pictorial and numerical information.

Track separation and association in different views via color is improved, if similar (e.g.close) objects have different colors (see color plate 3 and 5).

2.5. Colors on dark and light background

The color plates 6a,b,c show points of varying size on black, blue and white background. For the representation of small points, a rather dark background is preferable. However, a light background is often preferred for a variety of reasons. If points on a light background are surrounded by a thin dark frame (see color plates 6 d,e,f) their visibility is enhanced substantially. The color of small points surrounded by a white frame and drawn onto dark background is not perceived, i.e. the points seem to be white. For large objects however, a white frame improves recognition considerably, e.g. for blue objects on black background.

Due to the frame, the effective size of points or lines increases, which leads to a loss of resolution. This is overcome by drawing first all frames and in a second pass all points and lines. This is demonstrated in color plate 7 with a blowup of 4 tiny points drawn on black and white background without frame (a), drawn sequentially, i.e. frame, point, frame, point ... (b), and drawn in two passes (c). Experience shows, that resolution is not decreased in this way, but in high density regions a black background is preferred.

The methods described until now lead to a picture as seen in color plates 3 and 5, which are fairly easy and fast to understand.

3. Visual Analysis

In most experiments a large number of events are recorded on computer storage devices. It is often necessary to examine visually a subset of these events for a variety of reasons, as e.g.:

- check of hardware and software (on- and off-line)
- check of selected events,
- intuitive understanding of events,
- search for suitable events for talks and papers.

The examination should be effective and unbiased. However, one cannot assume that the intuitive impression one gets from the picture is right, in contrast to the situation, where one is looking at a picture presented in a talk or paper. One may be mislead for several reasons:

- loss of information,
- false assumptions,
- suggestive results.

In short: what looks good, may be wrong.

In the following we will discuss a variety of different pictures, which might help to avoid misinterpretations. Starting with representations of two dimensional data we will concentrate then on how to represent three dimensional data.

3.1. Use of picture transformations

It is common use in physics, particularly when handling multi-dimensional data, to apply suitable non-cartesian projections in order to better visualize the data, e.g. transverse versus longitudinal momentum, P_T/P_Z, which corresponds to ρ/Z in coordinate space. The choice of these projections depends strongly on the data to be displayed. A well known example is the application of logarithmic scales. It may be regarded as a non linear picture transformation and is particularly powerful for the examination of exponential curves, which are linearized (compare figures 4a and d) taking advantage of the fact that human perception can better judge and extrapolate straight lines than curved ones. In contrast to the original picture in figure 4a, the change of exponent is clearly visible in the logarithmic representation of figure 4d.

It will be shown below that segments of circles (tracks) can be linearized by a φ/ρ projection, as seen in figure 4b and e. Through subsequent linear transformations it is possible to enhance features, which are otherwise difficult to extract (see the kink in figure 4e and c). These and similar methods will be discussed in the following.

3.2. Helices in Cartesian and Angular Projections

Due to the radial event structure and the cylindrical detector structure it is of interest to investigate the use of angular projections, i.e. of projections based on cylindrical and spherical coordinates. The most famous of such projections is the Mercator projection, which deals with the spherical structure of the earth. The ρ'/Z projection discussed above may also be regarded as an angular projection.

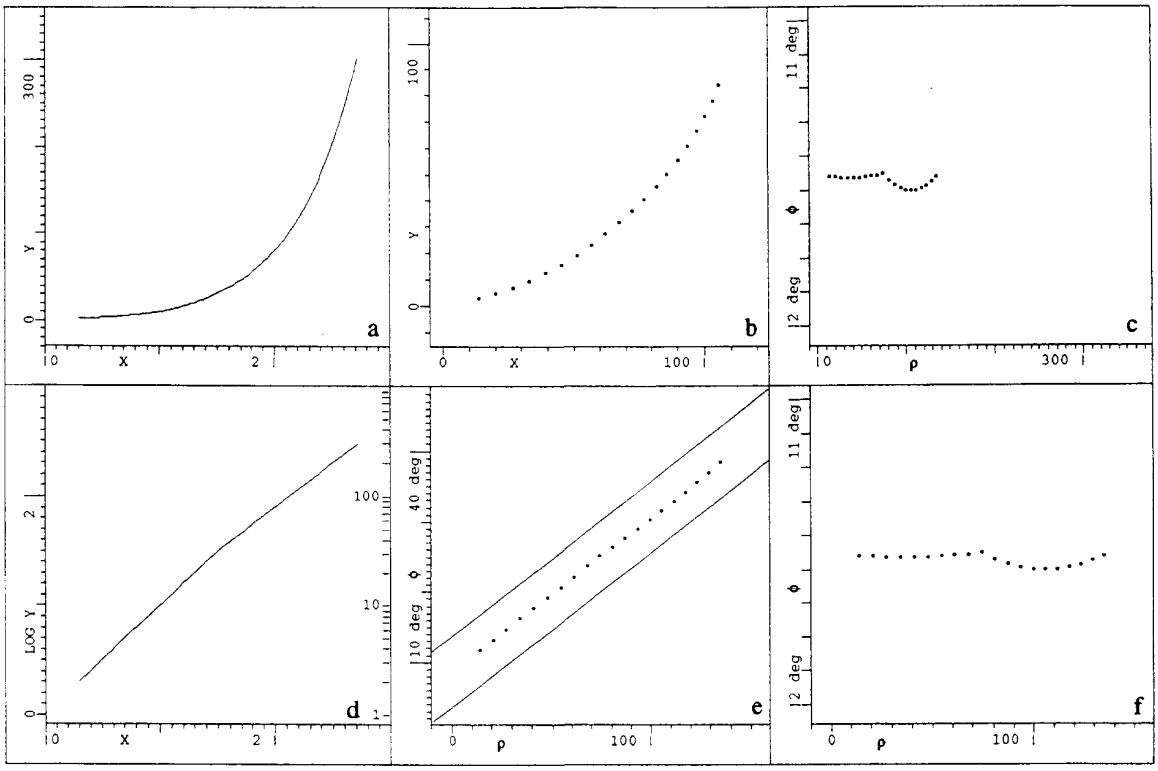

Fig.4 Linearization of an exponential curve and of a segment of a circle
a) exponential curve b) segment of a circle c) compressed φ / ρ
d) same curve as (a) in log. scale e) same segment as (b) in φ / ρ f) linear transform. of φ / ρ

In many detectors, such as the LEP detectors, tracks of particles are recorded, which move in a homogeneous solenoidal magnetic field parallel to the Z-axis. These tracks are described by helices. In order to better understand the use of angular projections, the helix equations will be formulated in cylindrical and spherical coordinates.

Neglecting multiple scattering, charged particles of momentum $\vec{P} = [P_X\, P_Y\, P_Z]$ passing through a solenoidal field move along helices. If they start from the collision point at the origin of the coordinate system, the helices can be described in a parametric form as function of $\Delta\alpha$:

$$X = cP_T[\cos(\alpha_0 + \Delta\alpha) - \cos\alpha_0]$$

$$Y = cP_T[\sin(\alpha_0 + \Delta\alpha) - \sin\alpha_0] \qquad (1)$$

$$Z = cP_Z\Delta\alpha \quad \text{with} \quad \alpha_0 = \varphi_0 + 90° \;,\; \varphi = \varphi_0 + \Delta\varphi \;,\; \Delta\alpha = 2\Delta\varphi$$

and $\tan\varphi_0 = \dfrac{P_Y}{P_X}$, $P_T = \sqrt{P_X^2 + P_Y^2}$, $P = \sqrt{P_X^2 + P_Y^2 + P_z^2}$, $\tan\vartheta_0 = \dfrac{P_T}{P_Z}$.

The constant c depends on the magnetic field. Using spherical coordinates defined as:

$$\tan\varphi = \frac{Y}{X}, \qquad \rho = \sqrt{X^2 + Y^2} \;,\; R = \sqrt{X^2 + Y^2 + Z^2} \;,\; \tan\vartheta = \frac{\rho}{Z}$$

one gets: $Z = 2cP_Z\Delta\varphi$, $\rho \approx 2cP_T\Delta\varphi$, $R \approx 2cP\Delta\varphi$, $\vartheta \approx \vartheta_0$ (2)

by approximating $\rho = 2cP_T\sin\Delta\varphi$

Most particles have a sufficiently large momentum to justify the approximation, i.e. their track radius is sufficiently large.

Figure 5a shows 6 tracks in *Y/X*, where a helix gives a circle, the radius of which is proportional to P_T. The *Y/Z* projection of the same tracks leads to cycloids as seen in figure 5b. It can be seen from the equations (2), that under the above approximations, helices are linear in the angular projections φ/Z (5d), φ/ρ (5e) and φ/R (5f). Their inverse gradient is proportional to P_Z, P_T, and P respectively. In ρ'/Z (fig.5c) they are straight. In projections where any variable is drawn versus ϑ, e.g. φ/ϑ (5g), one gets approximately straight, vertical lines. The approximation fails for helices which do not pass through the center and for helices with many turns as can be seen in figure 5. As long as a helix with many turns passes again through the Z-axis, it is described in φ/Z by a set of parallel straight lines (see figure 5d). Particle momentum and charge cannot be estimated from the projections *Y/Z*, ρ'/Z and φ/ϑ.

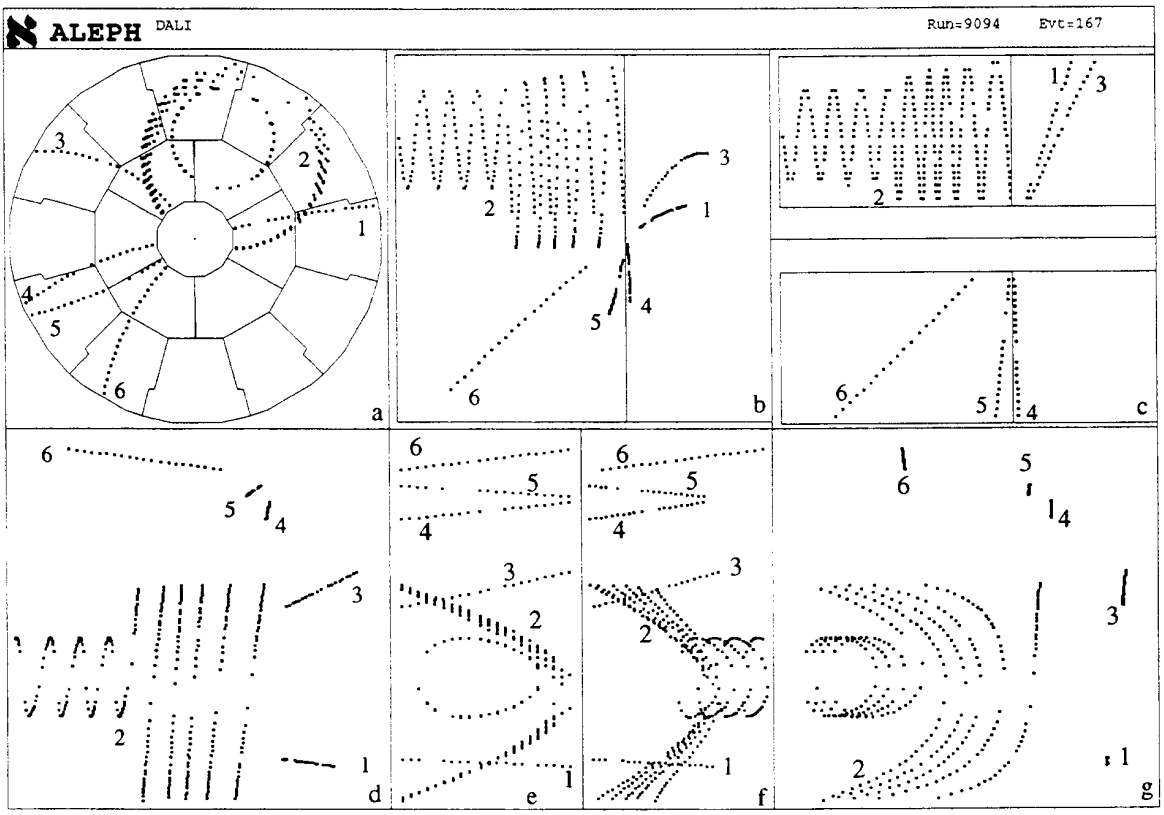

Fig.5: Helices in cartesian and angular projections

a) *Y/X* b) *Y/Z* c) ρ'/Z
d) φ/Z e) ϕ/ρ f) φ/R g) ϕ/ϑ

The φ/ρ projection is particularly useful to extrapolate tracks into the barrel part of calorimeters, whereas φ/Z is the best projection for extrapolation into the endcap part. This is due to the fact, that in projections of any variable versus ρ the barrel parts of different detectors are separated on the picture, whereas in anything versus Z the endcaps are separated, so that the rules of chapter 2.1 can be applied. φ/Z is preferable to *Y/Z*, as the longitudinal momentum

P_Z and the charge of the particles can be estimated.

3.3. Lines through Sequences of Points

In the pattern recognition programs the hits belonging to a track are searched for and a helix is fitted to them[1]. In color plate 8a three helices are drawn suggesting the existence of three independent tracks. The helices were derived from a fit to the hits seen in 8b, which shows that two of the tracks belong together, as incoming and outcoming track from a decay of a charged particle, yielding a so called "kink". Color plate 8c shows in another example a set of hits, which were joined by the pattern recognition program to two tracks, shown as lines. Although this assignment looks very convincing, it turns out to be less obvious, if only the hits are drawn (8d). A better way to show the hits together with their track assignment while avoiding the suggestive force of lines is to color the points according to their track assignment(8e).

The examples above demonstrate, that it is necessary to recognize tracks from their hits only. Therefore we need to understand how human perception connects a sequence of points to lines.

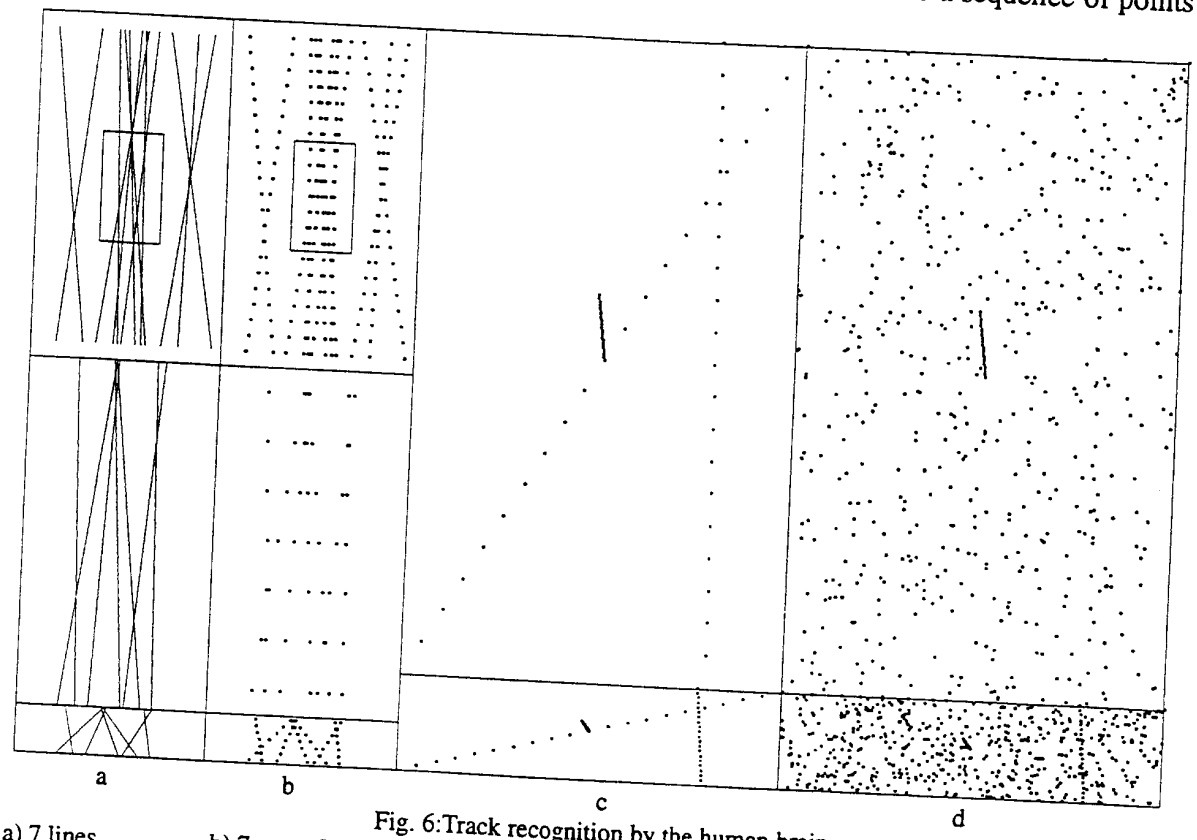

Fig. 6:Track recognition by the human brain

a) 7 lines same, blown up and compressed

b) 7 sets of points same, blown up and compressed

c) 3 sets of points compressed

d) 3 sets of points with noise compressed

To this purpose figure 6a displays 12 artificial, straight lines and in figure 6b the same lines formed of a sequence of points. In the blowup (6a) of the crowded center region seven lines are easily distinguished. However, if the lines are drawn as a sequence of points and

1. In reality the fit may take into account multiple scattering leading to a curve which is only approximately a helix.

blown up (6b), the seven lines are hardly identified. If, however, the picture is compressed in the direction of the lines (see bottom of figures 6b), the lines are easily identified, even if only drawn as points.

Figures 6c,d show the same 3 straight lines of rather different direction and length in a clean (6c) and a noisy (6d) environment, where the two long lines with large spacing between neighboring points are lost. Compressed pictures are shown at the bottom of these figures. In the noisy environment, the line in the direction of the picture compression is easily identified, contrary to the two other tracks, of which the long one was not compressed and the short one was "over compressed".

One learns from this exercise, that human perception identifies a sequence of points as lines by joining close points together and not by following - like a computer - a predefined mathematical function.

In the case of events of radial structure, there is no preferred direction of compression if one wants to visualize the total event (see figure 7a). However, there are methods of radial compression, e.g. the fish eye view (see figure 7b). The principle of such methods can be summarized as follows: the angle under which a point is seen from the center remains unchanged, but its distance from the center ρ is changed via a suitably chosen function to $\rho_{NEW} = F(\rho)$, e.g. $\rho_{NEW} = a + b\rho$ with $a > 0$ and $0 < b < 1$.

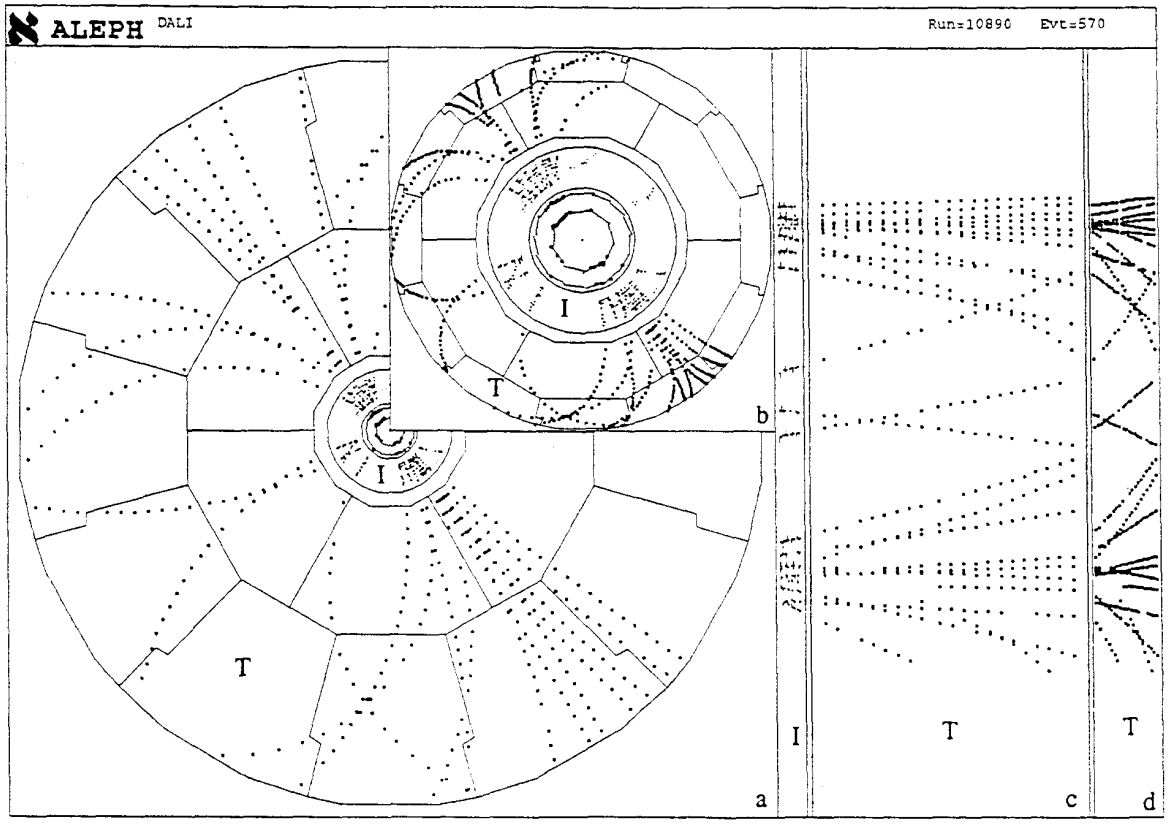

Fig.7: 2π compression of a total event in the ITC(I) and the TPC(T)
a) Y/X b) fish eye compression c) φ / ρ d) compressed φ / ρ

A more powerful method consists in "unrolling" the picture to the φ/ρ projection (see figure 7b) and compressing it (see figure 7c) in ρ direction.

If only a section of the events is to be visualized, there are other methods, which will be discussed below.

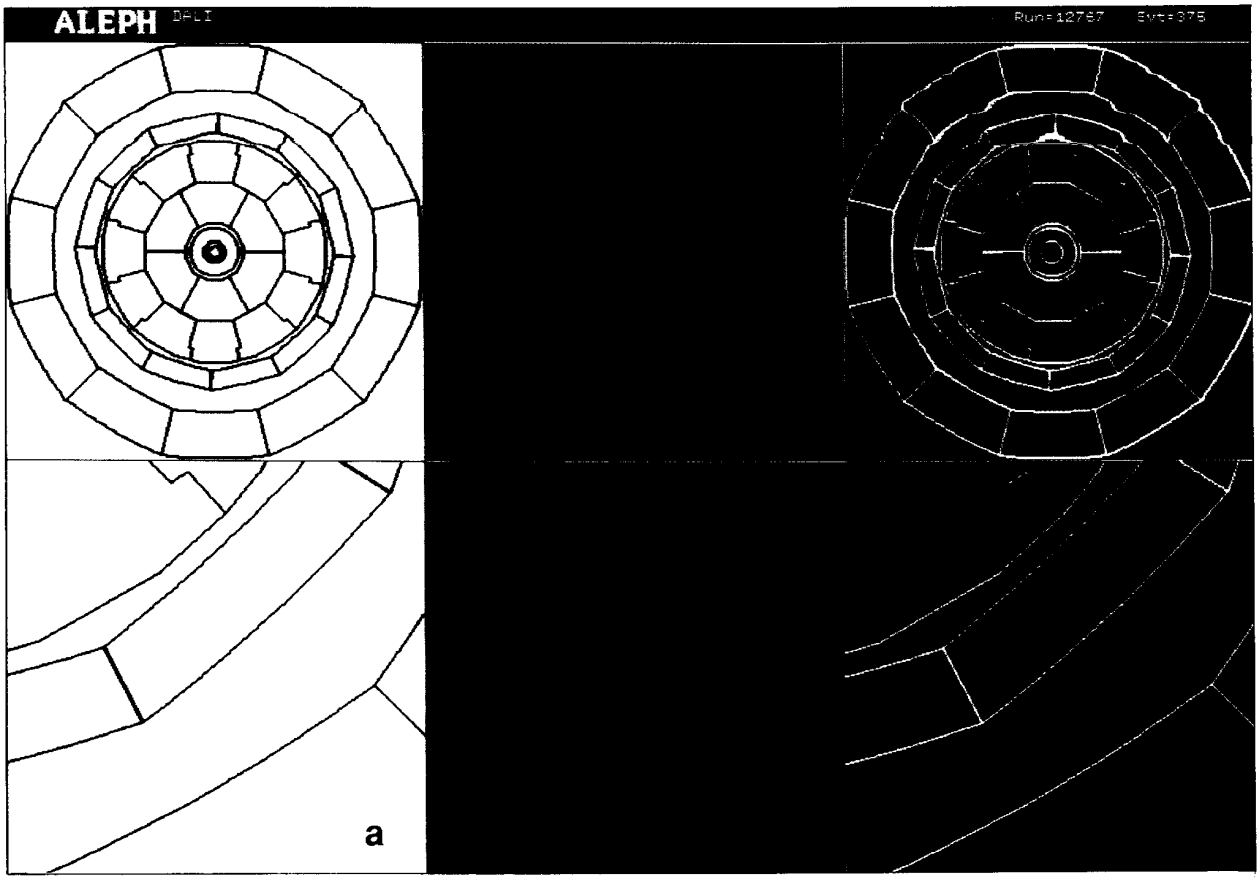

Color plate 1: Different ways to draw a detector

a) wire frame b) colored areas c) colored areas + wire frame

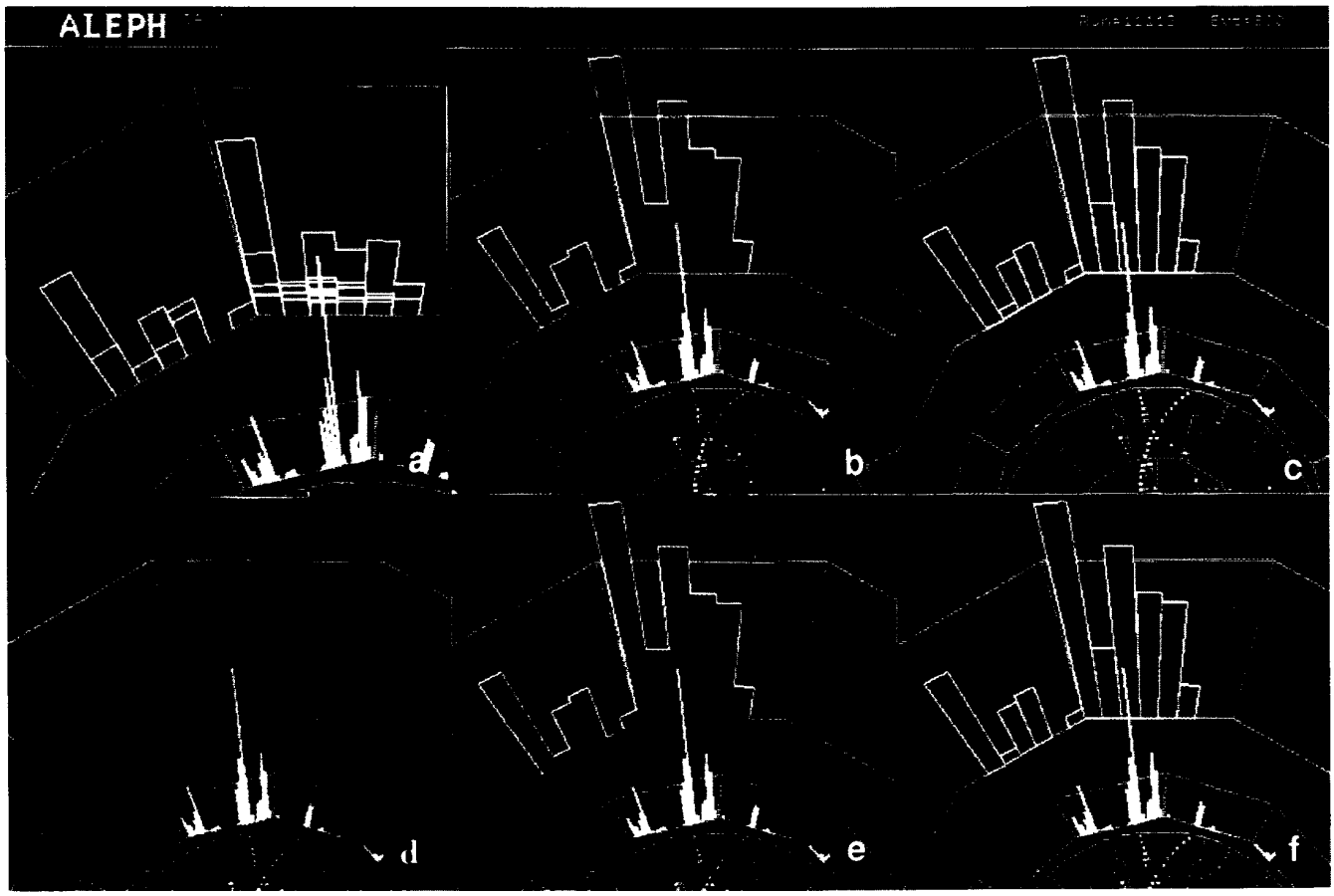

Color plate 2 : Skyline (a) and radial histograms (b-f) of energy deposits in a calorimeter

a) Skyline b) wire frame c) structured wire frame

d) unframed area e) framed area f) structured area

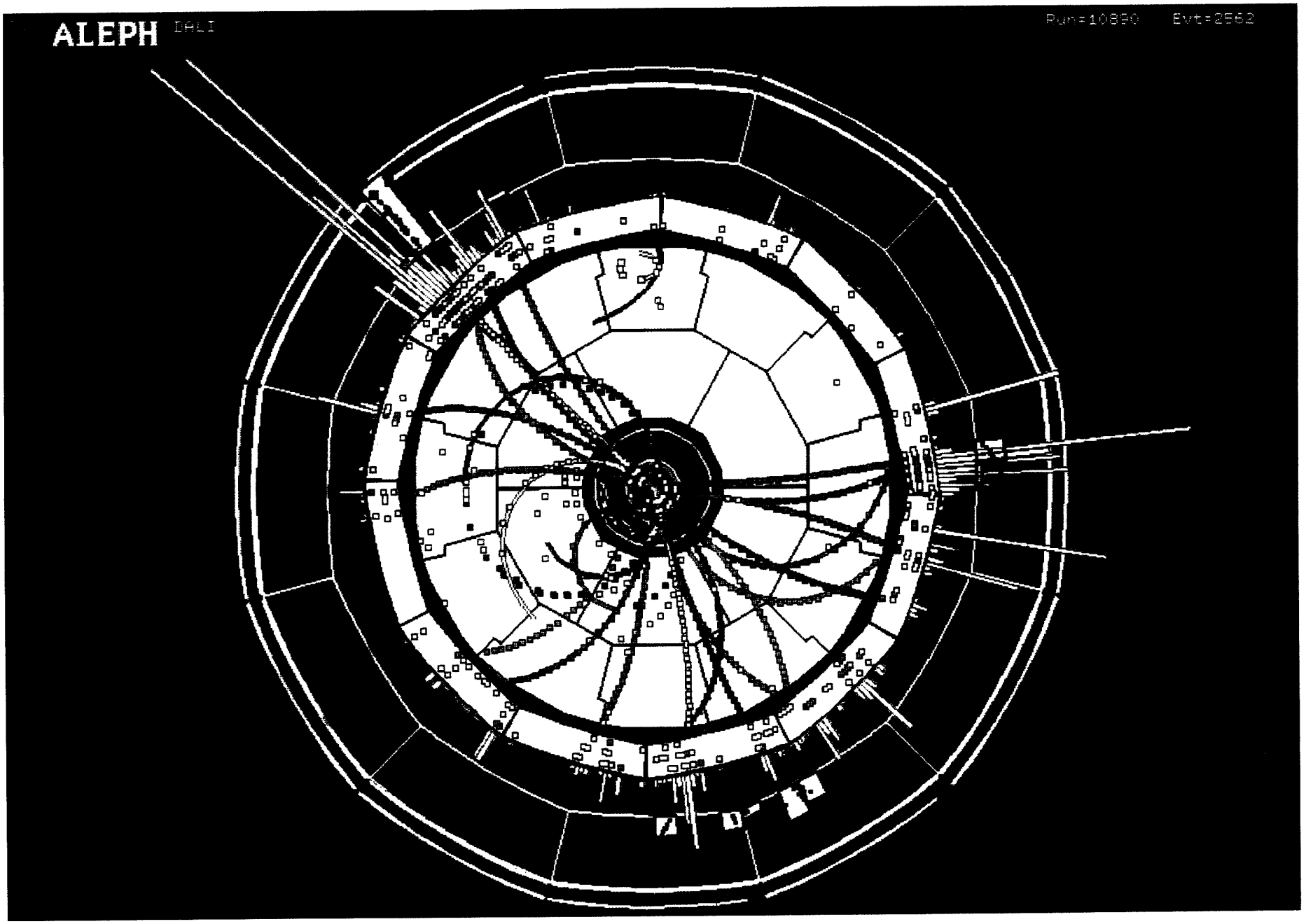

Color plate 3: Front view with fish-eye transformation (the same event as in color plate 5)

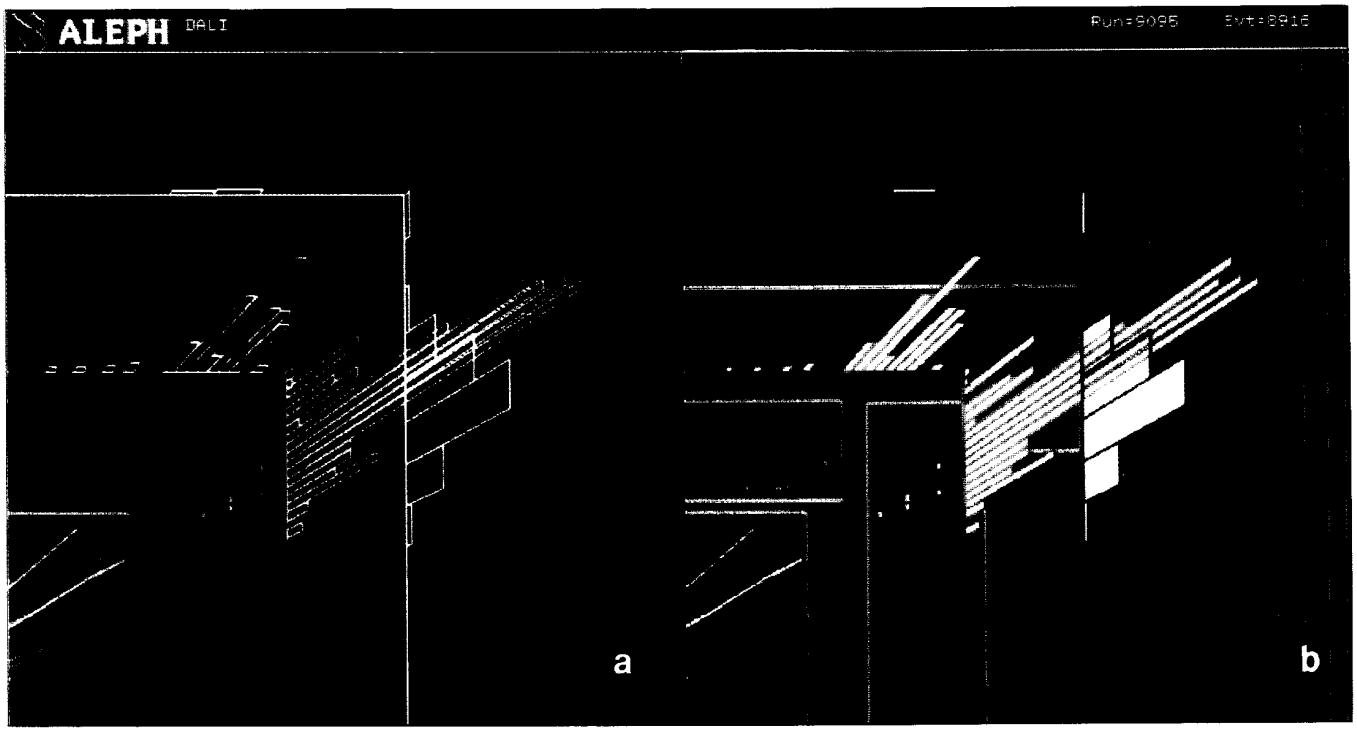

Color plate 4: Overlapping radial histograms in ρ'/Z

a) wire frame

b) structured areas drawn in the sequence:
histogram 1, histogram 2, wire frames of histogram 1.

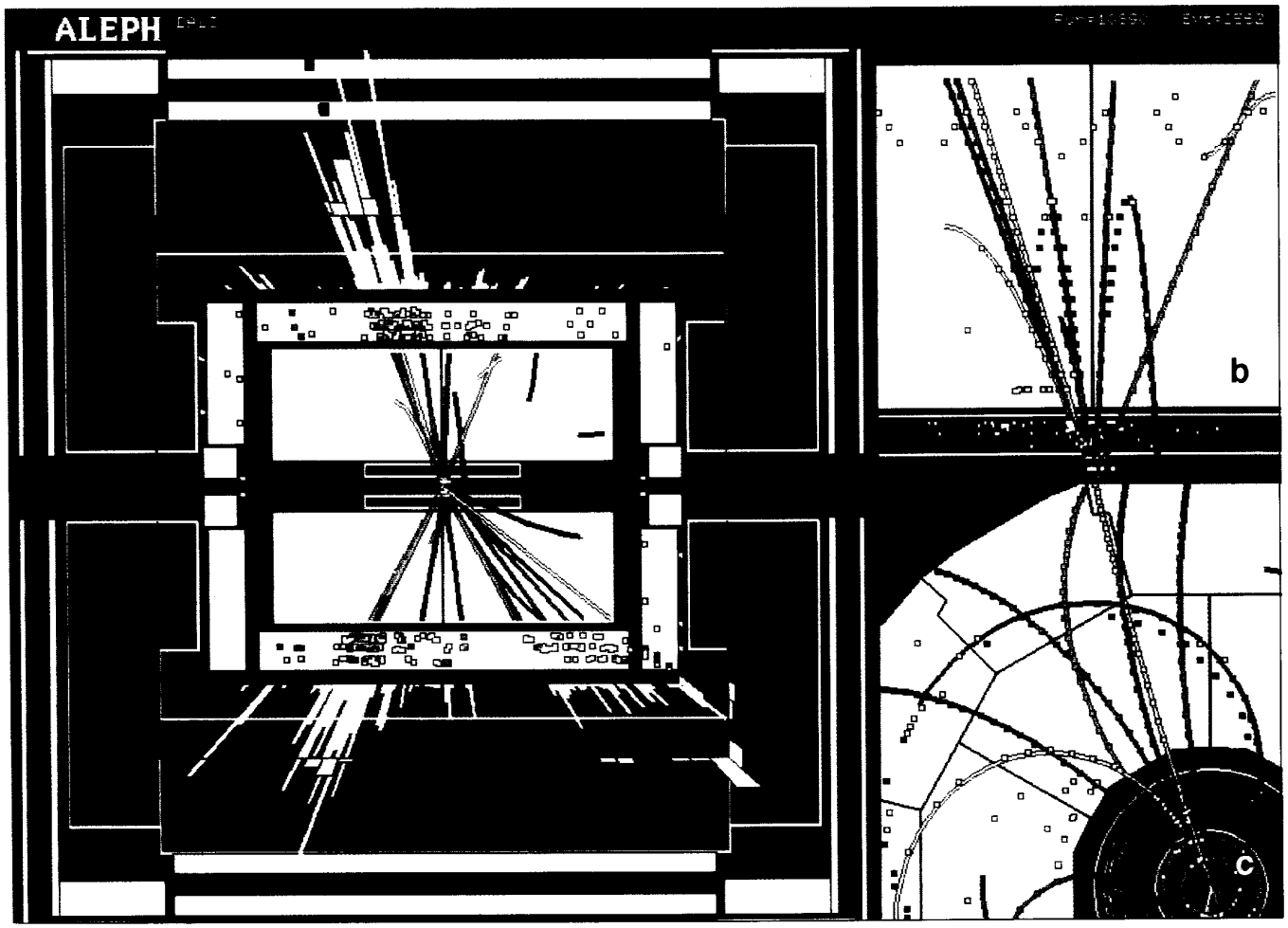

Color plate 5: Use of colors to separate and correlate tracks for the event shown in color plate 3

a) ρ'/Z

b) Section of the TPC and the inner detectors in ρ'/Z

c) Section of the TPC and the inner detectors in Y/X

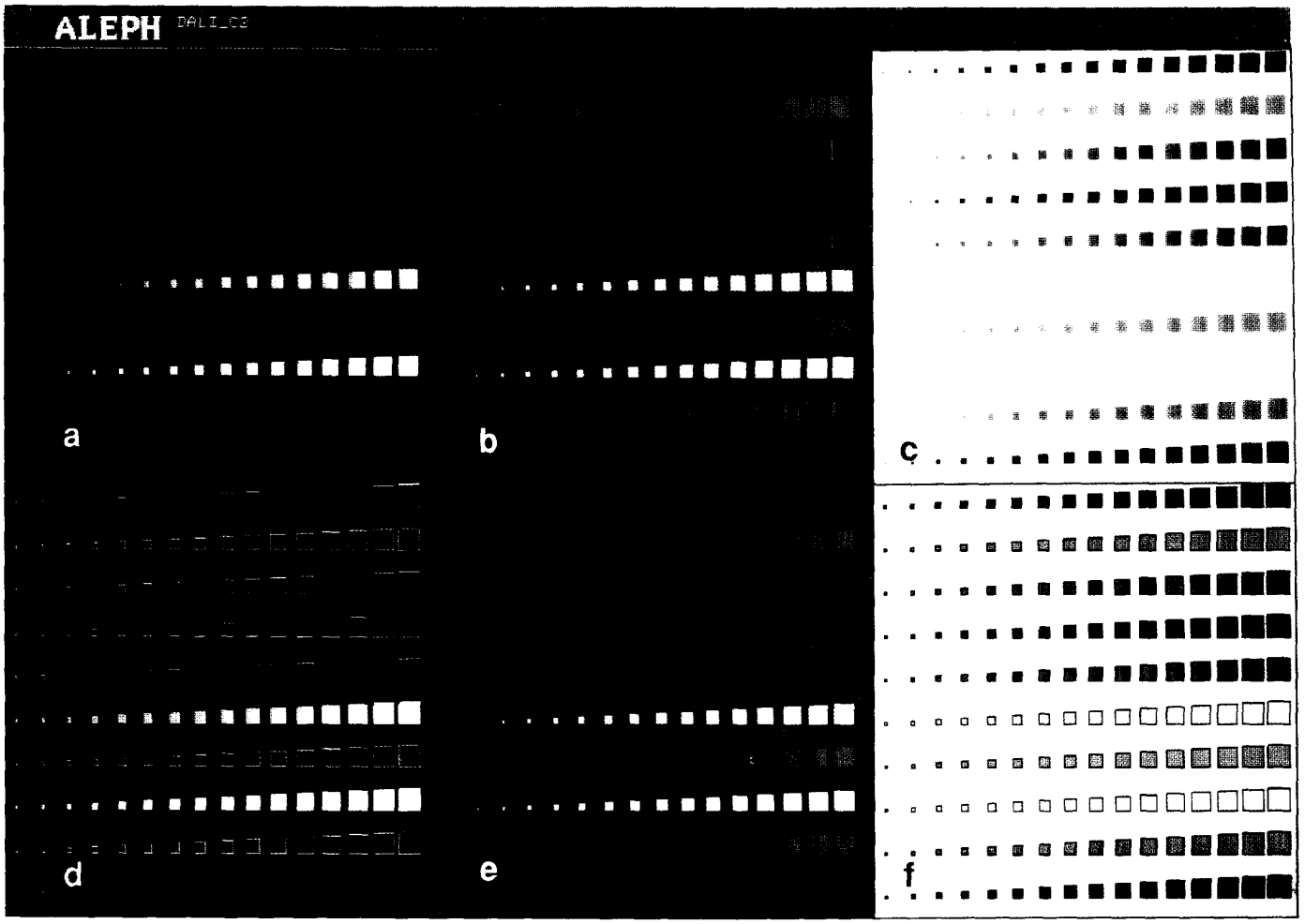

Color plate 6: Points of different size on black, blue and white background

a) without frame on black b) without frame on blue c) without frame on white

d) with frame on black e) with frame on blue f) with frame on white

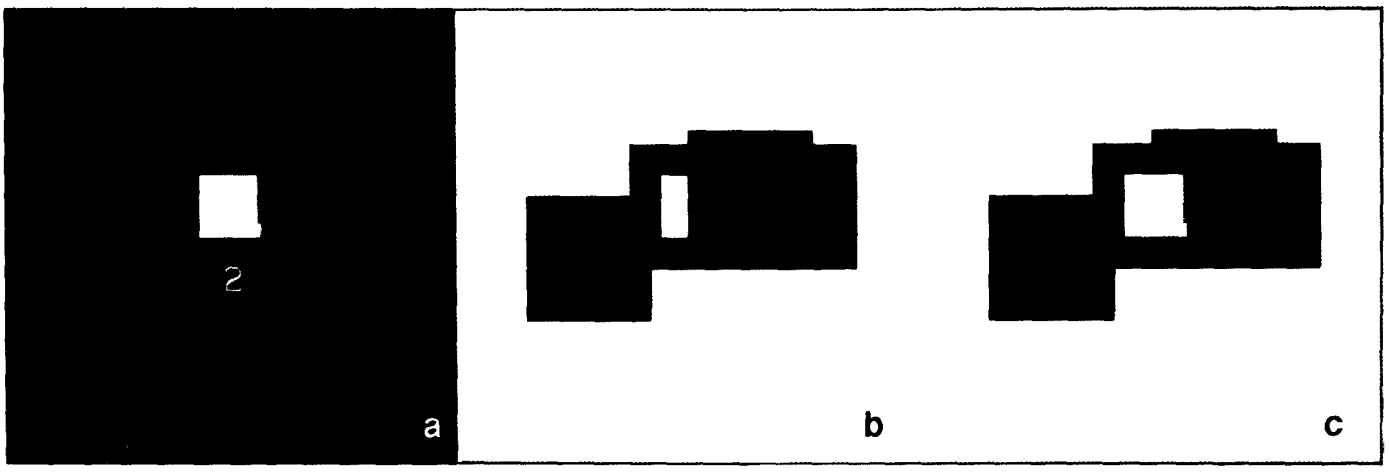

Color plate 7: Various ways to draw (framed) points in the sequence 1, 2, 3, 4

a) unframed points on black b) points and frames drawn together: c) all frames drawn first and then all points

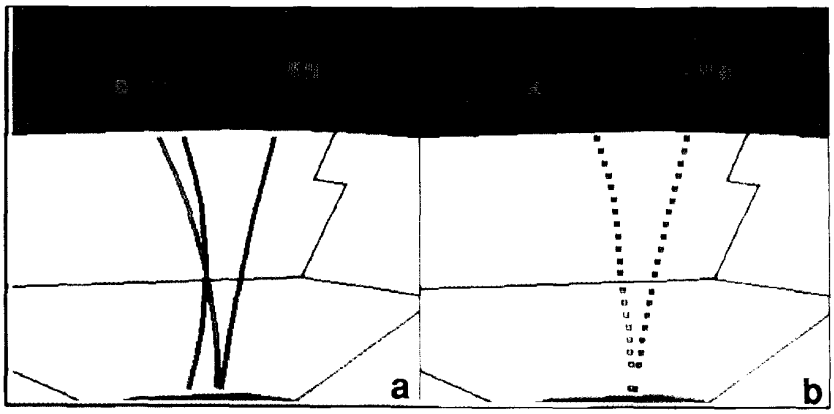

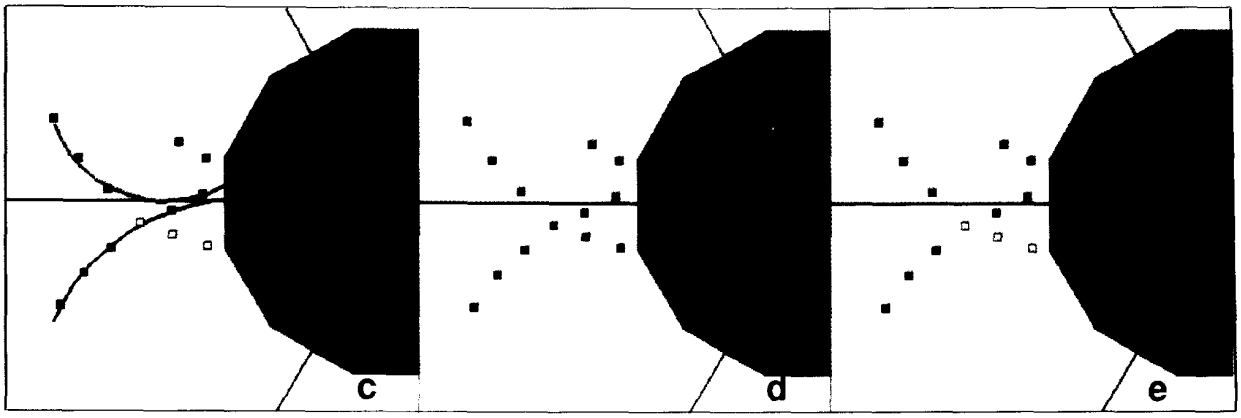

Color plate 8: Tracks drawn as lines or as a sequence of points with different color schemes

a) lines
b) points with track dependent color
c) lines + points with track color
d) points is one color
e) points with track color

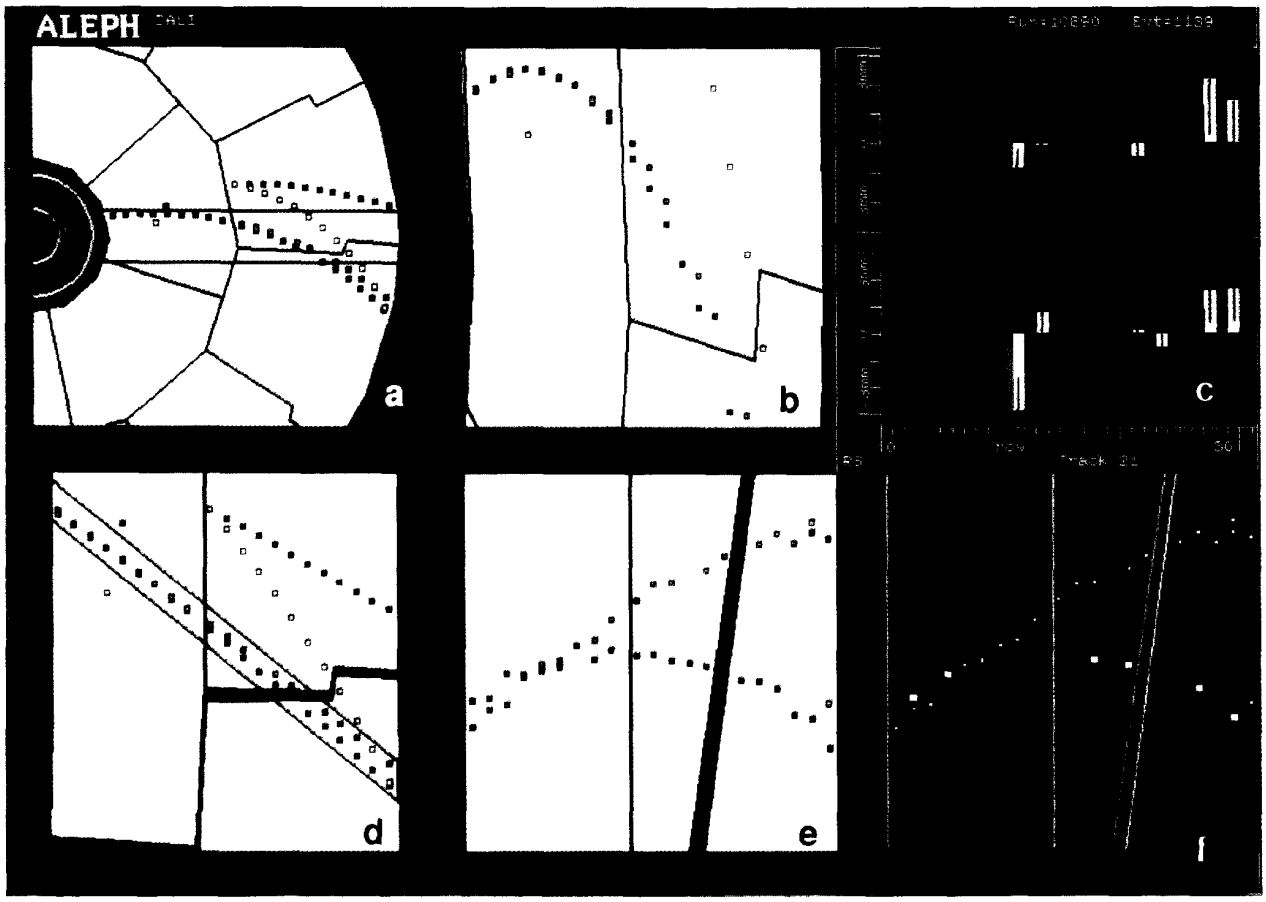

Color plate 9: Methods to blow up single tracks

a) Y/X with aspect ratio ≈ 1
b) Y/X with aspect ratio ≈ 6
c) residual plot, above: Y-X-plane
d) φ/ρ
e, f) linear blow-up of φ/ρ
f) hits colored as in (c)

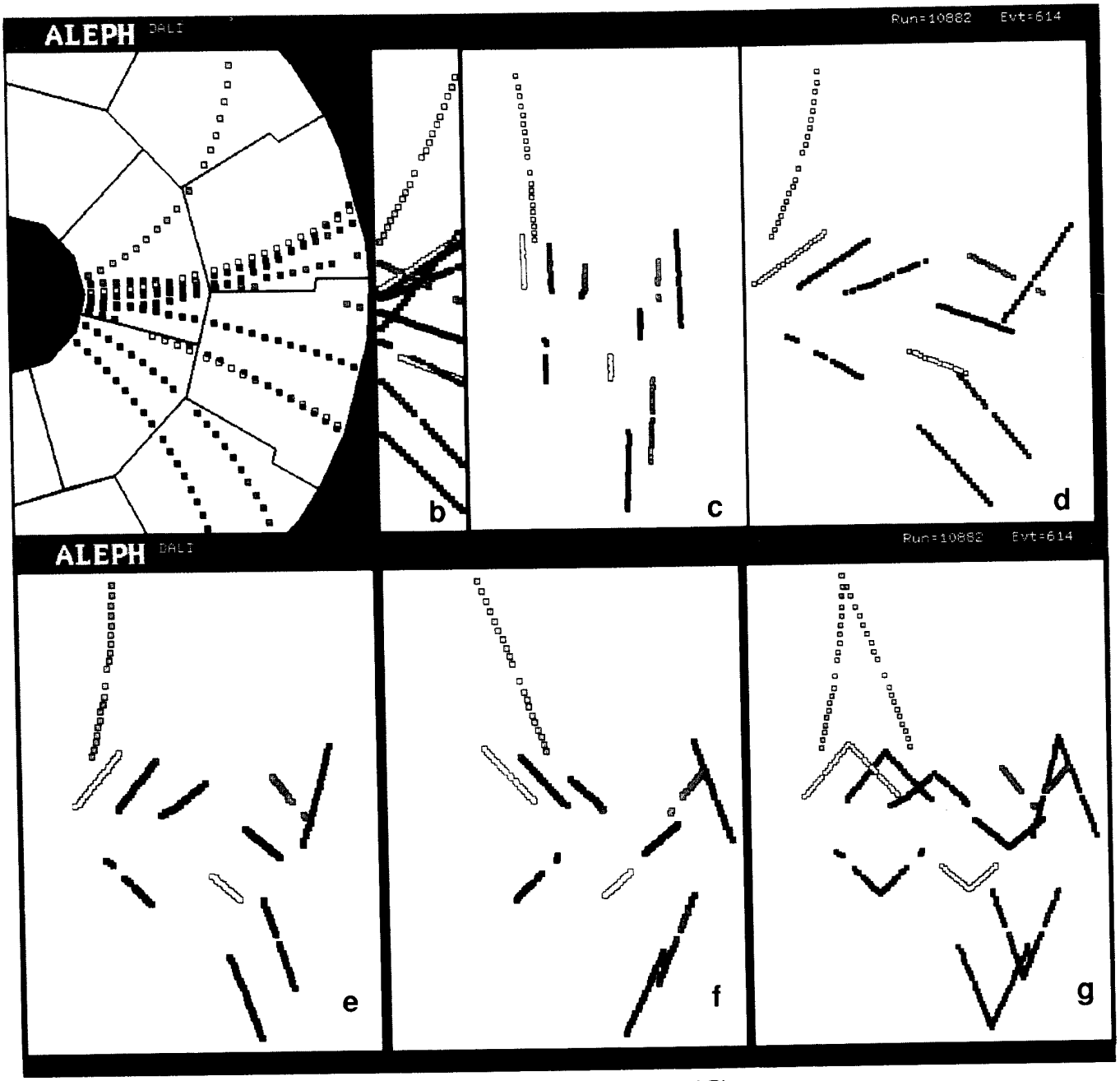

Color plate 10: From Y/X to the V-Plot

a) Y/X
b) compressed φ/ρ
c) φ/ϑ
d) $\varphi/(\vartheta+kD)$
e) $\varphi/(\vartheta+kD)$
f) $\varphi/(\vartheta-kD)$
g) $\varphi/(\vartheta\pm kD)$

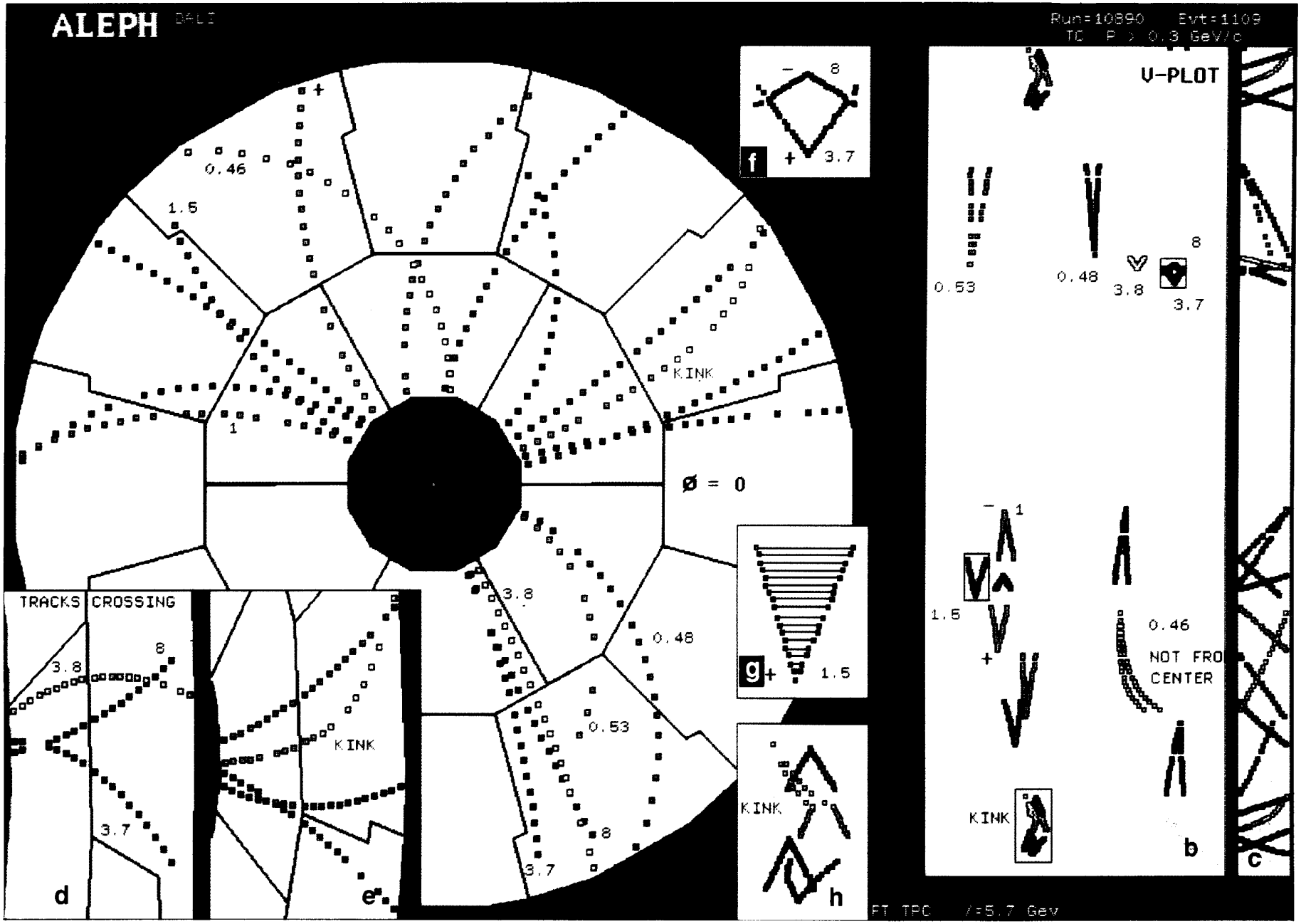

Color plate 11: How to use the V-Plot

a) Y/X

d,e)Y/X, blown up and rotated from (a)

f, g, h } V -Plots, blown up from (b)

b) V -Plot

c) φ/ρ

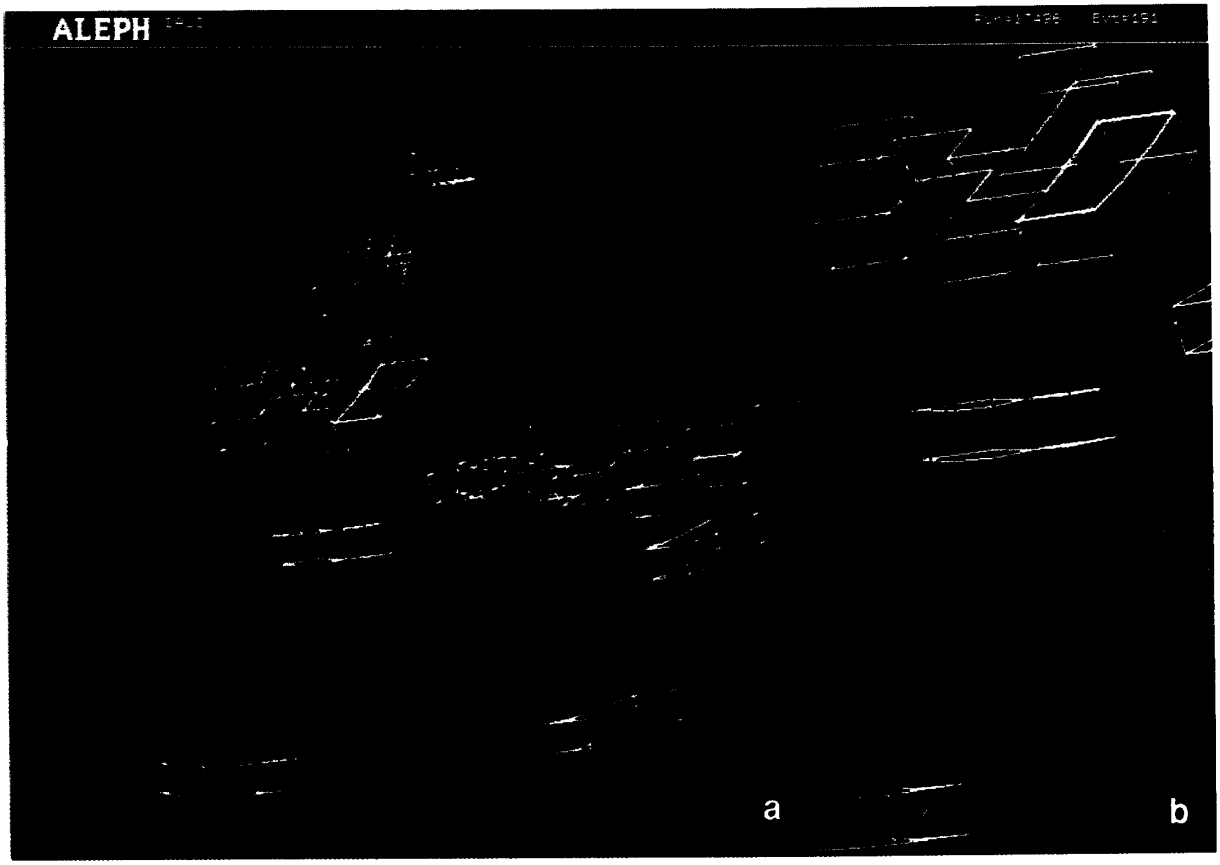

Color plate 12: Active cells of the SICAL (blue, pink = clusters 1, 2, yellow = noise) as wire frames
a) perspective projection b) blow-up of a section of (a)

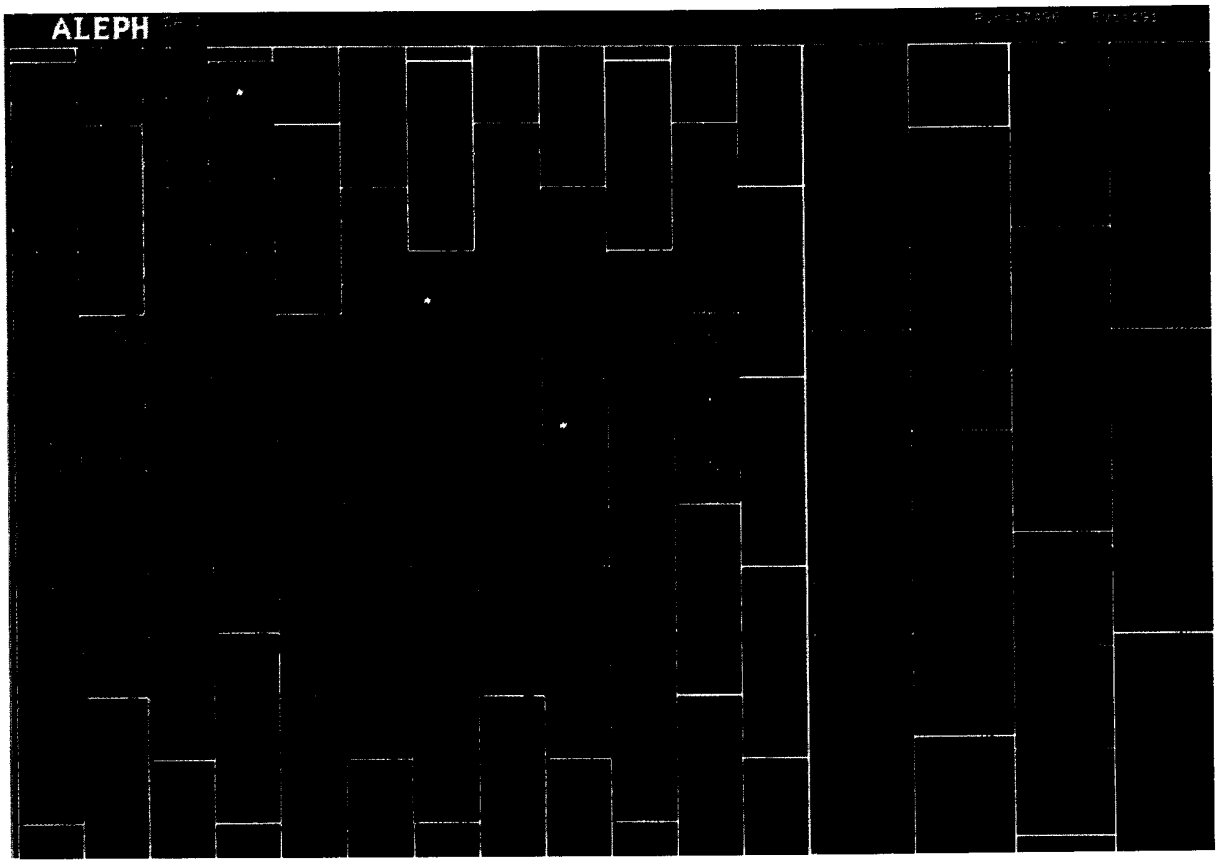

Color plate 13: The same active cells of the SICAL as shown in color plate 12
a) Puzzle Plot b) blow-up of a section of (a)

3.4. Blow-up of a sequence of points

In many detectors hits are recorded with very high precision. In the ALEPH TPC hits are recorded with a sampling distance of $d = 60\ mm$ and a precision of $\Delta = 180\ \mu$. In order to visualize errors of this size on a screen, one must blow up the interesting part of a picture such that 1 pixel corresponds at least to 180μ As a consequence a screen image with 1000 x 1000 pixels covers only a detector area of 180 x 180 mm^2 in the case of a symmetric magnification (*aspect ratio = 1*). Therefore one ends up with only very few points on the screen, i.e. one looses the relevant context to all the other hits of the track. This gets even worse for detectors of higher precision.

If one is only interested in the errors perpendicular to the track direction, a small magnification in track direction and a high one perpendicular to it (*aspect ratio > 1*) yield a picture, on which many hits are visible as well as their deviation from a smooth track. Color plate 9a displays a section of *Y/X* with *aspect ratio = 1*. The rectangle shows a section, which is blown up to give the picture in color plate 9b with an aspect ratio defined by the sides of the rectangle.

However, if tracks are rather curved, as is the case in color plate 9a, they can only be contained in a correspondingly large rectangle, which means, that the magnification perpendicular to the track is limited. This can be overcome by first linearizing the track using φ/ρ (9d) followed by a sufficiently large linear transformation. As an example, the parallelogram[1] containing the tracks as seen in color plate 9d is transformed to the full size of the square picture (9e), where the scattering of the hits is now clearly visible.

So a magnification can be reached (9e and f), which yields a picture similar to a residual plot (9c, upper part). The residual plot, however, has the disadvantage not to show tracks or hits close by. Note the use of colors to associate the hits between color plates 9d and f.

In essence it turns out that through such methods the limits due to the resolution of the screen and of the human visual system can be overcome.

3.5. Visualisation of the Vertex Region

It is sometimes required to blow up track images near to the vertex region, e.g. for the investigation of secondary vertices close to the vertex. This can be accomplished by a linear blowup or by use of the fish eye transformation (see chapter 2.2), which allows to visualize the tracks further away from the centre. Close to the vertex, i.e.in the region of interest, it yields a picture similar to a linear blowup, so that distances and correlations can be estimated correctly.

3.6. Imaging Events from Fixed Target Detectors

In many detectors, particularly in fixed target detectors, particles leave the interaction point in a preferred direction. Two questions, arising when visualizing such events, will be discussed here:

- How to estimate visually, by which amount straight tracks point beside the interaction point? This problem arises in experimental setups, where tracks are curved by a magnetic field but recorded in a detector further down outside the magnetic field.

---

1. The parallelogram and the rectangle are defined interactively using the rubber band technique.

- How to show tracks in small subdetectors close to the center and large subdetectors further downstream simultaneously?

Figure 8a shows a simulation of hits recorded outside a magnetic field. The amount by which the tracks point beside the interaction point is a function mainly of the particle momentum, which is of main interest. However, due to the large distance of the hits from the interaction point it is rather difficult to estimate this quantity from the picture without relying on a pattern recognition program providing straight lines for backward extrapolation as in the bottom of figure 8a.

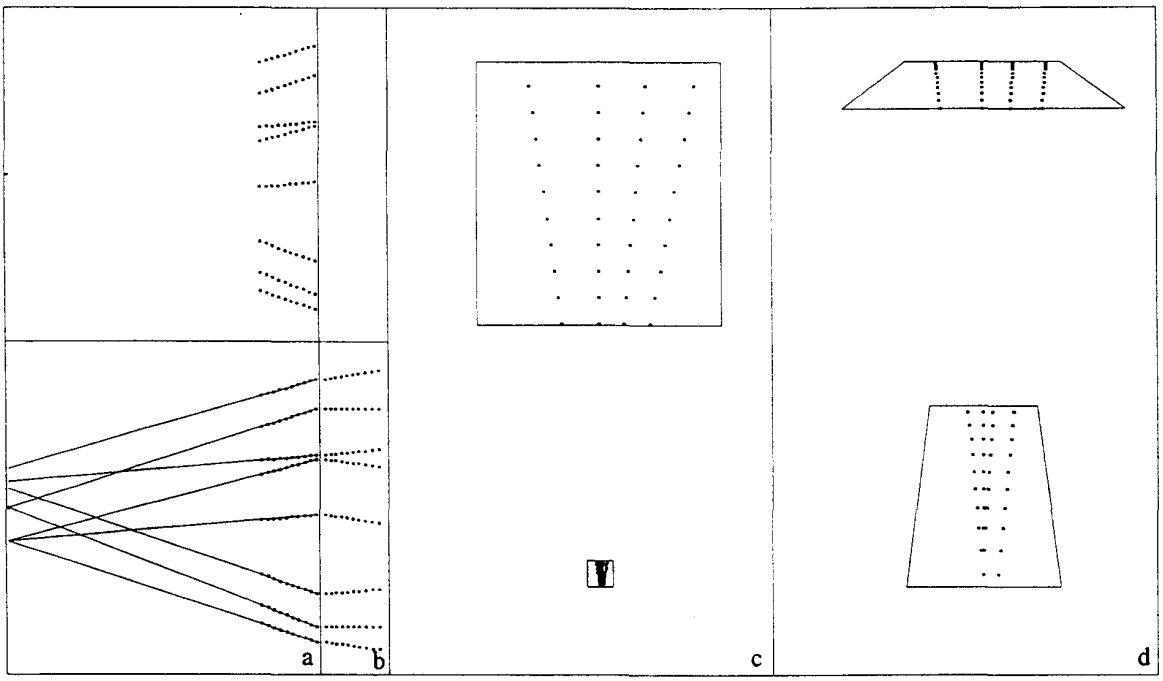

Fig.8: Non linear transformations of straight track segments
a) Y/X b) Y'/X' c) X/Y d) X''/Y''

The tracks can be described by $Y = a + bX$, where X is the downstream axis. As mentioned above, the offset, a, depends mainly on the particle momentum and only very slightly on the track direction, unlike the gradient, b, which depends on both. The equation can be rewritten as $Y' = \frac{Y}{X} = \frac{a}{X} + b = aX' + b$. one sees that the non linear transformation $X' = \frac{1}{X}$, $Y' = \frac{Y}{X}$ transforms straight lines into straight lines. They are shown in Y'/X' in figure 8b[1]. From the gradient a of these lines the particle momenta can thus be locally estimated, i.e. from a picture showing only the hits without the center point.

By further application of linear transformations one can derive a more general formulation $X'' = \frac{X}{1+cX}$, $Y'' = \frac{Y}{1+cX}$, which again leaves straight tracks straight [2]. This transformation corresponds to the picture formed in our eye, when looking with a grazing view onto a flat image[2]. Figure 8c shows a picture - X/Y - from two subdetectors of very

1. The Y'/X' projection was properly scaled.
2. If $Y \ll X$, X can be replaced by ρ leading to the fish eye transformation discussed before.

different size with 4 straight tracks. In *X"/Y"* (8d) the tracks remain straight, but can be resolved in both subdetectors, and the track segments can be connected by a straight line. This transformation can also be applied to curved tracks. If only slightly curved, the track images are practically identical to those obtained from the fish eye transformation discussed before.

3.7. Island Representation of Calorimeters

Calorimeters are composed of cells, in which energy is deposited either by the traversing particles or by their showers. These cells may be grouped together in layers surrounding the inner part of the detector (see the three layers of points in the outer ring shown in figure 9a). The optimal projection for the representation of these layers depends on the geometrical structure of the calorimeter. The electromagnetic and hadronic calorimeters in ALEPH have a projective structure, i.e. neighboring cells of different layers can be grouped into towers, the axis of which points to the center of the detector, as well for the barrel as for the endcap. This suggests the use of φ/ϑ to display single layers, as:

- barrel and endcap can be shown on the same picture,
- pictures of different layers have the same geometrical structure.

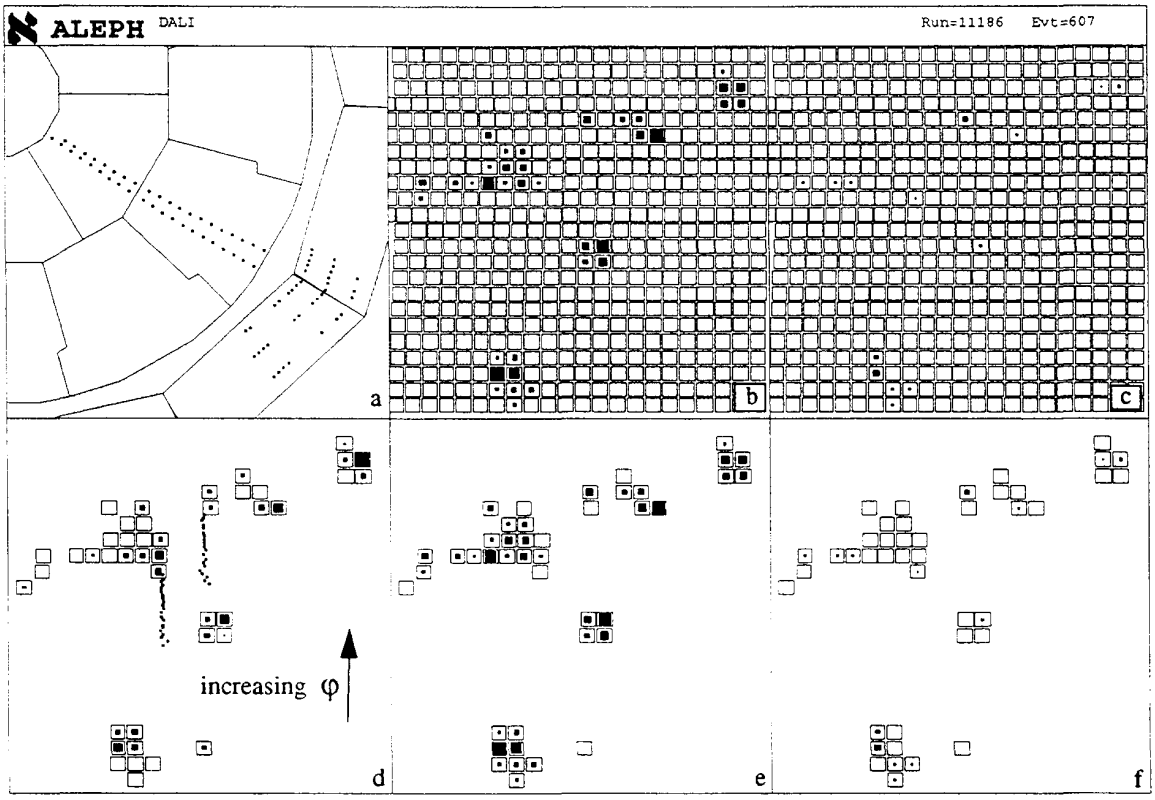

Fig: 9: Display of tracks and calorimeter data in Y/X (a) and φ / ϑ (b-f)

a) Y / X
b) Full structure of layer 2
c) Full structure of layer 3
d) Island structure of layer 1 and TPC tracks
e) Island structure of layer 2
f) Island structure of layer
The area of the squares is proportional to the deposited energy.

In figure 9a hits lying in a given solid angle are shown. The same hits are shown in φ/ϑ for layer 2 and 3 in figures 9b and 9c, respectively. The amount of deposited energy per cell is proportional to the size of the squares inside the cell. In order to analyze the shower development between these two layers, the active cells - cells with deposited energy - in layer 2 must be compared to the corresponding ones in layer 3. This is facilitated considerably, if

only towers are drawn, which have active cells in at least one of the three layers (see figures 9d,e,f) [3]. This yields an irregular, island like substructure identical in all three images, which helps to correlate the cells in the different layers.

The next problem is how to associate tracking information to the calorimeter information, i.e.tracks to showers. In *Y/X* shown in figure 9a, the track to shower correlation is not obvious, due to the missing *Z*-information and to the overlap of showers lying behind each other. If φ/ϑ is used instead, two methods may be applied:

- A track fit is made to the tracks, and the entry point into the first layer is displayed. In this case one relies on a good track recognition and fit. The direction under which particles enter the calorimeter is not visualized.
- The hits of the TPC are superimposed in a φ/ϑ projection onto the first layer (see figure 9d). This method is rarely used, as further information is needed for an unambiguous analysis. In this representation there is no information, if the azimuthal angle φ increases or decreases for the tracks, e.g. if the right track seen in figure 9d is associated to the island above or below. For this and other reasons it is necessary to use additional projections and reliable methods of track correlation between the different projections.

Particle momentum and charge cannot be estimated from φ/ϑ. This problem and the difficulties when applying the second method, are caused by the fact that only two dimensional projections are applied. In the next chapters possible solutions to represent the full three dimensional information will be discussed.

4. Three Dimensional Representations for Visual Analysis

Many (sub-) detectors record the position of hits in three dimensions. Here we will assume, that the errors of all three measured coordinates are sufficiently small, so that patterns of tracks or showers can be meaningfully visualized in any projection.

For the representation of such data we will try to find single pictures or picture sets, which allow to extract all relevant information.

Several methods are used to solve this problem:

- perspective projections, sometimes called 3D,
- volume rendering, shading etc.,
- smooth rotations on appropriate 3D-stations,
- stereo pictures,
- technical drawings showing front, side and top views,
- unconventional methods applicable for special sets of data.

The application of these methods for visual event analysis will be discussed in the following chapters.

4.1. Perspective Projections

Figure 10a shows a two dimensional wire frame projection of two objects, which we interpret as being three dimensional objects. In doing so, we apply more or less strictly a set of assumptions, namely

- Straight lines on the picture are straight in space.
- Each line represents one line only, i.e. it is not composed out of several lines, overlaid or just touching on the projection.
- Lines parallel on the picture are parallel in space.
- Lines touching each other at a corner, touch each other in space.
- The angles between lines at the corner are angles of 90°.
- Several discrete line segments lining up on the picture do so in space.

As a consequence we see two cubes in figure 10a. But there exists an infinite number of three dimensional objects, which yield the same two dimensional image. One such object, for which the above assumptions are not fulfilled, is seen in figure 10b which is obtained from 10a by a rotation of 20° around a vertical axis in the picture plane. If we see a picture like the one in figure 10a, we prefer automatically the most familiar solution. However, we can only be sure that this interpretation is right, if we know beforehand, that the above assumptions are valid, or if we know beforehand, that we see two cubes.

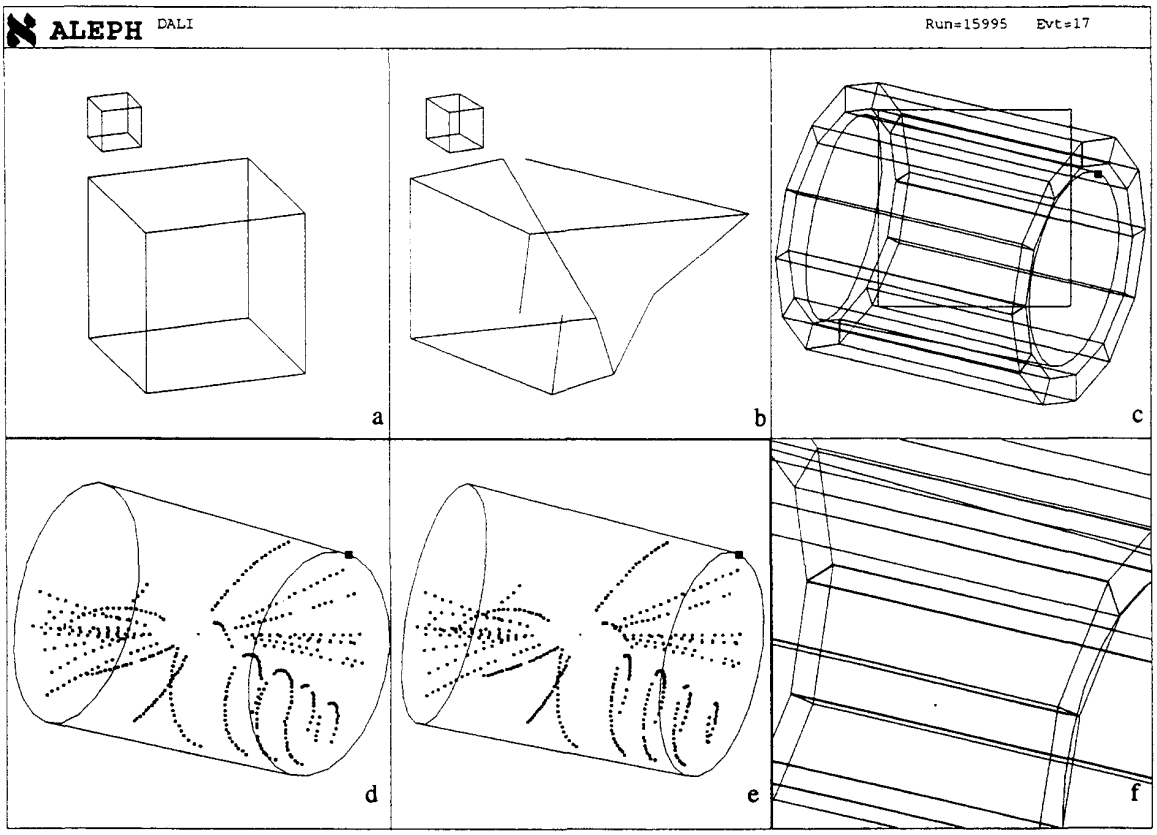

Fig.10:Perspective projections of
a) two "cubes" b) two "cubes" rotated by 20° c) TPC + ECAL
d) TPC + event (left eye) e) TPC + event (right eye) rotated by 6° f) TPC + ECAL blown up

If we know, that what we see is a cylinder, we can reconstruct a three dimensional cylinder in our brain from a two dimensional projection of it. Therefore, a two dimensional projection of a detector, of which we know what it looks like, will form a three dimensional image in our brain (see figures 10c,d,e).

However, if we look at points, at lines or at an event, no one of the above assumptions is valid a priori. For an event there is no way to estimate the depth of points and tracks (see figure 10d), i.e. the picture of the event remains two dimensional. Furthermore, one may be mislead by basing a decision on the preference of the simplest solution, which is even reinforced, if a two dimensional projection of hits and tracks is combined with a three dimensional detector image. An exception are points (e.g. confirmed end points of tracks) from which we know, that they lie on a plane. If this plane is surrounding a volume, one gets two solutions, one for the front and one for the back plane.

The advantage of showing the detector lies in the fact, that the direction, from which we are looking, is visualized. Furthermore one transmits the information, that the data are three dimensional.

A problem arises, if a part of the picture is blown up in a way that the lines, which compose the cubes, the cylinders etc., are unconnected. In this case the assumptions above, even if valid, cannot be applied, so that a rather complicated picture results (see figure 10f).

In the case, that the event and not the detector is of main interest, we can conclude that, what is often called 3D, is in reality a 2D projection not able to convey all relevant information. There are classical methods to improve this situation, namely the combination of perspective projections with

- shading and volume rendering,
- smooth rotations,
- stereo pictures.

They will be discussed in the following.

4.2. Shading and Volume Rendering

The picture of an event consists of

- points and lines, representing hits and tracks, which must be kept thin, in order not to loose resolution for the display of many of them, and of
- rather small boxes representing calorimeter cells, where often cells lie behind each other.

In the first case volume rendering techniques cannot be applied as we cannot distinguish enough intensities or colors on small objects. In the second case the wire frame technique must be applied if cells should not be obscured. This excludes shading and volume rendering.

If shading and volume rendering are applied to several subdetectors surrounding each other, one is lead back to cut away perspective views, onto which a two dimensional projection of an event can be overlaid, but the event picture and the underlying detector picture do often not correspond to each other. One may find simple events which allow this, but for visual analysis, which has to handle all events, these methods seem not to be applicable.

4.3. Smooth rotations

One of the best methods to get additional information about three dimensional objects from a two dimensional display is a smooth rotation. During rotation the three dimensions of the data, their horizontal and vertical picture position *(H,V)* and their depth *(D)* are mapped onto *H,V* and the speed of displacement, i.e. onto three independent variables.

When applying a small smooth rotation, it is possible to identify hits, tracks or track segments, which are close to each other, as they move with similar speed. However a rotation of about 6^o, as between figures 10d and 10e, leads to a displacement $\Delta \approx \frac{D}{10}$, i.e. the precision by which we can estimate the depth position is reduced by one order of magnitude. In many cases this is insufficient, e.g. the curvature of a track bent in the rotation plane can hardly be judged.

If one rotates by 90°, the errors of Δ and D become compatible. In this case one gets a smooth transition between two views, which helps to associate the images of hits and tracks on the first view with their corresponding images on the second one. However, for high multiplicity events, this method of association becomes rather tedious. It will be shown in section 4.5, that three orthogonal views are needed in more complicated cases, i.e. rotations around different axes are required. Thus a thorough check of an event becomes time consuming and requires a fair amount of discipline from the operator.

4.4. Stereo Images

If we could look at the data, presented in one way or the other in real 3D, e.g.on a stereo device, we would be rather pleased to easily understand the detector picture and the event structure and to be able to confirm the assumptions of section 4.1. The display of the detector image helps considerably, as it gives the necessary information of the depth scale. As each of our eyes is a 'two dimensional image recorder', smooth rotations help us to match the points and lines from the two images in our brain.[1]

However, stereo imaging suffers from the same deficiency as discussed in the previous chapter. Due to the relatively small eye distance as compared to the distance between our eyes and the objects, the depth precision, when looking at things, is considerably worse than the lateral precision. This is even true, if the objects are reduced in size and projected close to us. Again, we are unable to judge the curvature of a track, if it is curved in a plane through our eyes. These observations are easily confirmed with real objects.

From the figures 10d and 10e one gets a stereo image, if one succeeds to look at the left picture with the left eye and the at the right picture with the right eye. One may estimate by comparing the two images the tiny differences, which lead us to see a stereo image.

4.5. The Method of Technical Drawings

A commonly used method of representing three dimensional objects is found in

1. Colors do not help the matching, as stereo recognition in our brain uses the intensity information of the pictures only. Proofs are found in the literature [4] and by the fact, that our stereo vision is not deteriorated, if images are artificially presented to the left and the right eye with different colors for identical objects.

technical drawings, where three orthogonal projections are used, normally the top, front and side view. In figures 11a,b,c five specially selected tracks are shown in *Y/Z*, *Y/X* and *X/Z*. Apart from a small change in length, the group of three tracks (1,2,3) gives the same image in *Y/Z* and *Y/X*, whereas they look very different in *X/Z*. Apart from a rotation in the picture plane, the images of the two isolated tracks are practically the same in *Y/X* and *X/Z*, but are different in *Y/X* and *Y/Z*.

For a thorough check of a track - or a set of nearly parallel tracks - two projections are required, one where the track is seen curved and one where it looks practically straight. In the case of an event, where tracks go into many directions, at least three projections are required, as in the example above. This means that the event must be rotated around several axes.

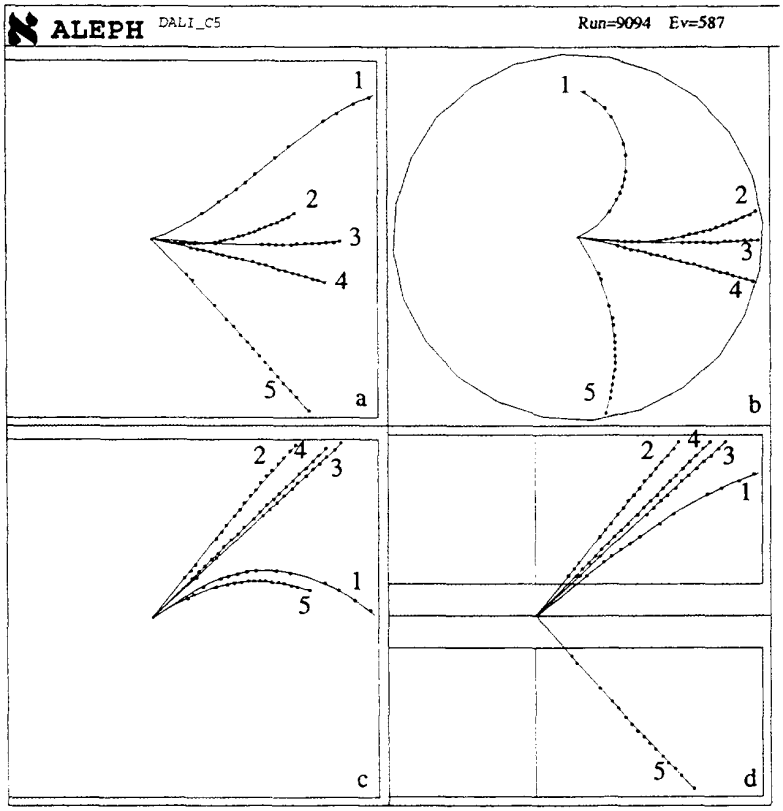

Fig. 11:Top, front and side view and ρ'/Z of five selected tracks

a) Y/Z b) Y/X

c) X/Z d) ρ'/Z

However, *Y/X* (figure 11b) and the non linear ρ'/Z projection (figure 11d) show all tracks either from the curved side or from the straight side, respectively. This is due to the fact that a track looks straight in Y'/Z with $Y' = Y\sin\alpha + X\cos\alpha$, if α is chosen such that the track lies approximately in the picture plane, which means $Y' \approx \rho'$. Therefore, the top, front and side view can be replaced by the two orthogonal projections *Y/X* and ρ'/Z. This is due to the fact that all tracks point to the same center.

However, very close to the center, the radial event structure is normally broken due to measuring errors, so that the interpretation of ρ'/Z becomes difficult. It should be further kept in mind, that momentum conservation cannot be checked in this projection.

Even the use of two projections instead of three suffers from the fact, that one has to

associate hits and tracks in one picture to their image in the other one. Therefore, it will be tried in the following to show ways of presenting three dimensional data in one picture only, using unconventional but less intuitive projections.

For all methods of 3D data representations discussed so far, it is difficult to find solutions of simultaneous data compression of the total event, as discussed in chapter 3.3 for 2D representations.

5. The V-Plot, a Three Dimensional Representation for Visual Analysis of Tracks

It is the advantage of conventional projections, that they can be applied to a large variety of objects and experimental setups. However, this is also their biggest disadvantage, as it is difficult to optimize them to special problems. In the following we propose projections, which were specially developed for the ALEPH experiment. We will discuss a picture called V-Plot, which was developed for helices, i.e tracks of particles moving in a homogeneous solenoidal field. We will then generalize the underlying principles and apply them to a different experimental configuration.

5.1. The Helix Representation via the V-Plot

It was shown in chapter 3.2 and figure 7d that tracks are better recognized in a compressed φ/ρ projection than in Y/X. This is shown again in color plates 10a,b. The compression facilitates the identification of tracks, but not their separation, as the total picture space is reduced as well (10b). The best track separation is obtained via ϕ/ϑ (color plate 10c). As discussed before, a representation in ϕ/ϑ does not allow to estimate charge and momentum, in contrast to ϕ/ρ, and it is not possible to verify, if tracks really enter and leave the chamber.

Therefore it is tempting to use a linear combination of the two projections, namely $\varphi/(\vartheta+k\rho)$. In color plate 10d, a slightly modified projection $\varphi/(\vartheta+kD)$ is shown with $D = \rho_{MAX} - \rho$, where ρ_{MAX} is the outer radius of the tracking device, here the TPC. The value of k is interactively chosen and scales the gradient of the straight track images. This projection conserves most of the good features of both projections, namely approximately straight track images, the ease of momentum and charge estimation as in φ/ρ and the good track separation as in φ/ϑ.

φ/ρ and φ/ϑ are two projections, which together represent the full 3D information of the data. They may be replaced by the two symmetric projections, $\varphi/(\vartheta+kD)$, introduced above, and $\varphi/(\vartheta-kD)$. If $k > 0$, they represent the full 3D information as well (see color plates 10e,f). As last step, the two projections are drawn on top of each other as seen in color plate 10g. The two superimposed track images of a single track form a V pattern, where the exit point, $D = 0$, lies at the tip of the V.

A somewhat modified definition of the variable D is more useful: $D = R_{MAX}(\vartheta) - R$, where R is the spherical radius defined above and R_{MAX} the distance of the outer surface of the tracking detector from the center in the direction of the hit, so D is the distance from the hit to the outer surface of the TPC in this direction. If the tracking detector is of cylindrical form,

R_{MAX} depends only on ϑ, i.e. $R_{MAX} = Min\left(\frac{\rho_{MAX}}{\sin\vartheta}, \frac{Z_{MAX}}{|\cos\vartheta|}\right)$, where the outer cylinder surface is given by ρ_{MAX} and $\pm Z_{MAX}$.

The interpretation of this so called "V-Plot", as can be derived from the equations 2 in chapter 3.1, is summarized in the following:

- V-position : $\phi,\vartheta \Rightarrow$ spatial track direction.
- V-direction : up or down $\Rightarrow$ particle charge.
  ALEPH: up $\Rightarrow$ negative, down $\Rightarrow$ positive charge.
- V-angle : $gradient \sim \frac{1}{P}$ = particle momentum^{-1}
  Wide V's $\Rightarrow$ high momentum,
  narrow V's $\Rightarrow$ low momentum.
- V-width : proportional to D, i.e. to track distance from exit.
  The tip of the V denotes the track exit.
- curved V-arms : the track has either low momentum or its origin is outside the center.

This means, that one can retrieve the full 3D information from the V-Plot. This is due to the fact, that two projections are superimposed. As the ordinate φ is the same for the two projections, a hit is represented by two points, which may be replaced by a horizontal line connecting them. Such lines have three degrees of freedom. Their center point gives φ and ϑ and their length is a measure of the distance of the hit from the outer surface of the detector, so that one could in principle recalculate the three original hit coordinates. The V-Plot is therefore a 3D representation of the TPC hits.

The V-Plot has a particularly high information content. However, one has to prove, that a human operator sitting in front of a terminal is able to work with these pictures, and especially, that the doubling of hits and of tracks does not give pictures, which are too complicated for visual analysis. Such an investigation cannot be done by theoretical arguments but by applying this technique to typical and difficult events.

5.2. Application of the V-Plot, Example 1

To illustrate how to work with the V-Plot in practice, *Y/X*, ϕ/ρ and the V-Plot are compared in color plate 11 showing an event, which was cleaned by eliminating all noise hits, i.e. hits, which were not associated to tracks by the pattern recognition program. When stepping clockwise, i.e. with increasing φ, through the tracks, one can compare the track representations in *Y/X* (11a) with those in the V-Plot (11b). This comparison is simplified by passing through the compressed ϕ/ρ projection in color plate 11c.

On color plate 11 several tracks are labeled by their measured momentum in [GeV/c] to demonstrate the relation between momentum and V-angle and to help the reader to associate the track images in the different windows.

Some special tracks are blown up in the inserts of color plate 11. The region around the track labeled "kink", is blown up from the V-Plot (11h) and from *Y/X* (11e). The kink is very pronounced in the V-Plot (11h) when compared to *Y/X* (11e). As this kink is mainly due to a variation of ϑ, it would be better visible in ρ'/Z, which is not shown here.

The V-arms of the blue track in insert (11h) and the V-arms of the yellow track in 11b are curved indicating that the tracks do not originate from the center.

The red V of the 1.5 GeV/c track is blown up in insert (g). The scattering of the points around a straight line is due to the limited precision of the measurements and multiple scattering. This demonstrates that one reaches a magnification, where the detector precision gets visible, so that one is neither limited by screen resolution nor by the human visual system.

The region around the 3.7 and 8 GeV/c tracks (red and blue) is blown up as *Y/X* (11d) and V-Plot (11f). The two tracks have one point in common, hence the two tracks cross in space, which cannot be unambiguously derived from *Y/X* (11d), as the depth of the hits is not represented. Many tracks crossing each other are found in *Y/X* (11a) but from the V-Plot (11b) one can derive, that no other tracks cross in space.

5.3. Application of the V-Plot, Example 2

A minor but rather helpful detail needs to be mentioned before discussing the next example. As $\vartheta = \text{atan}\frac{\rho}{Z}$ increases with decreasing Z for a fixed value of ρ, left and right would be inverted when comparing φ/ϑ with ρ'/Z. To avoid this, the ϑ-axis is defined as pointing to the left in the V-Plot and in all φ/ϑ projections. This is indicated in figure 12a by the arrows.

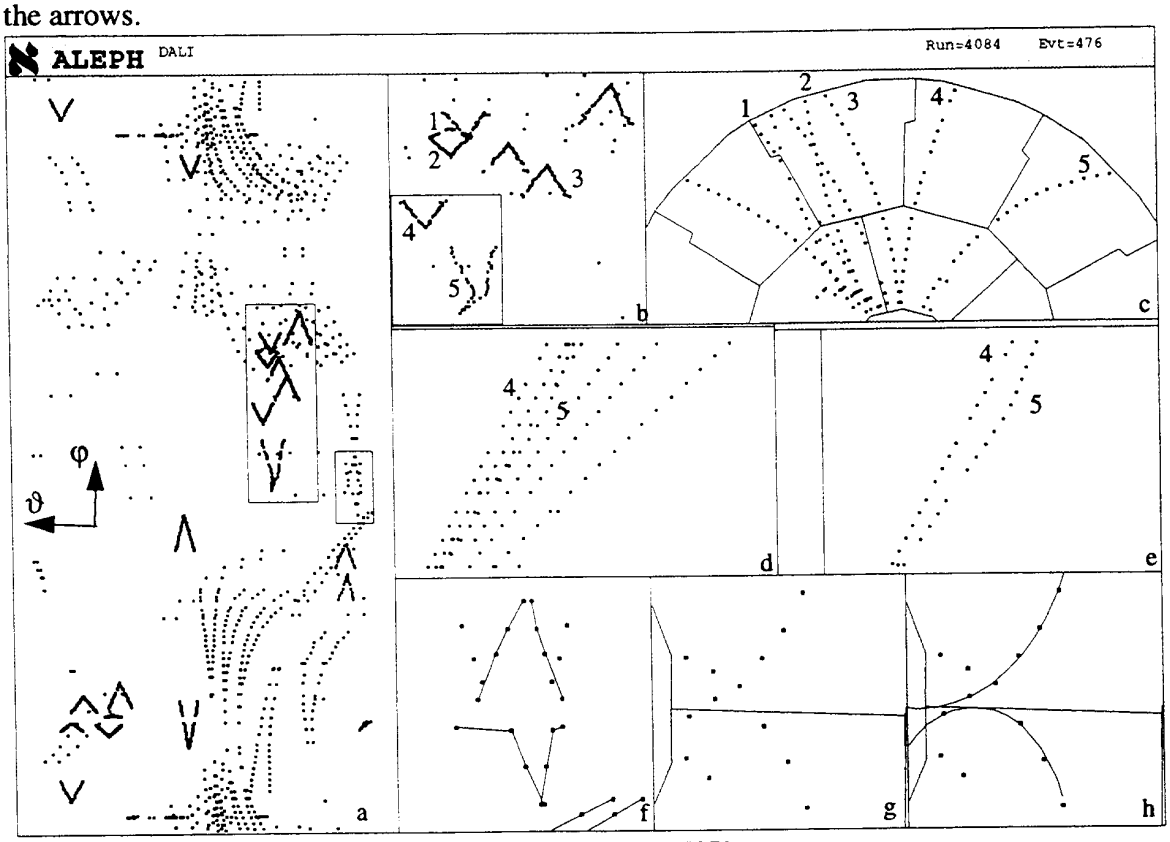

Fig. 12: Use of the V-Plot

a) V-Plot b) section of the V-Plot c) *Y/X*

d) ρ'/Z e) ρ'/Z cleaned

f) section of V-Plot with connected hits g) *Y/X* h) *Y/X* with hits and tracks

Figure 12a shows the measured hits (noise not removed) of the ALEPH TPC as V-Plot. The V-Plot provides a simple tool to select hits or tracks through a volume defined in position

and size via φ, ϑ and ρ. This volume can subsequently be visualized in other projections[1] or again as V-Plot, as is shown in the following examples:

- The angular section defined by the large rectangle (12a) is shown as V-Plot in 12b, as *Y/X* in 12c and as ρ'/Z in 12d,
- the angular section defined by the small rectangle in 12a is shown blown up in 12f and as *Y/X* in 12g,h,
- from the tracks seen in figure 12b, two are selected through the rectangle in this figure and shown as ρ'/Z in 12e.

The kink in track 5, which is due to the decay of a charged particle, is enhanced through the vertical compression of the V-Plot (12b) as compared to the kink shown in ρ'/Z (12e).

The blowup of the V-Plot (12b) shows a quadrilateral pattern typical for the decay of a neutral particle into a positive (2) and negative (1) particle. The corresponding tracks have a common origin in the TPC, i.e. away from the primary vertex. No other pattern of this form is found in 12a and 12b, i.e. no other decay of a neutral particle exists in the TPC. It is rather difficult to confirm that fact from *Y/X* and ρ'/Z.

The assignment of hits to tracks by the pattern recognition program, as indicated through the lines in 12f and 12h, looks rather unlikely in the V-Plot, where it is checked in 3D, compared to *Y/X*, where the depth information is lost (see also color plate 8c,d,e). The probably false association of the hits to tracks by the program may be due to the fact that the two tracks cross in space, as can be seen from 12f.

5.4. Extrapolation of Tracks via the V-Plot

In chapter 3.6 the φ/ϑ representation of calorimeter cells was discussed (see figure 9d). However no satisfactory method was found to associate the tracking data from the TPC to the calorimeter data. This problem is solved by use of the V-Plot.

Figures 13a and 13b show the front and side view of two tracks and those calorimeter hits, which lie in the same direction. The φ/ϑ projection of the three layers of active calorimeter cells is shown in figures 13d,e,f, where the shower development can be estimated easily, as discussed before. In figure 13c the V-Plot of the two tracks is superimposed to the calorimeter islands, so that the clusters created by the two charged tracks can be identified and the properties of the two tracks evaluated. If for some reason the last hits of a track are missing (which is not the case here), the exit position of the track can easily be deduced, i.e. even in this case tracks and showers can be correlated.

As seen in this example, the V-Plot is that representation of tracking data which is complementary to the most used display of calorimeter data, namely the Lego Plot.

The V-Plot is also applicable to backward extrapolations of tracks into inner tracking subdetectors, e.g. into a vertex detector, as long as three dimensional data are recorded. However, backward extrapolation via the V-Plot may lead to very complicated pictures, when getting too close to the vertex. This is the case if tracks do not point precisely to the vertex due to measuring errors, secondary decays etc., so that the variation of φ and ϑ gets very large.

---

1. The angles are interactively defined by use of a rubber band cursor, the values of ρ are preset.

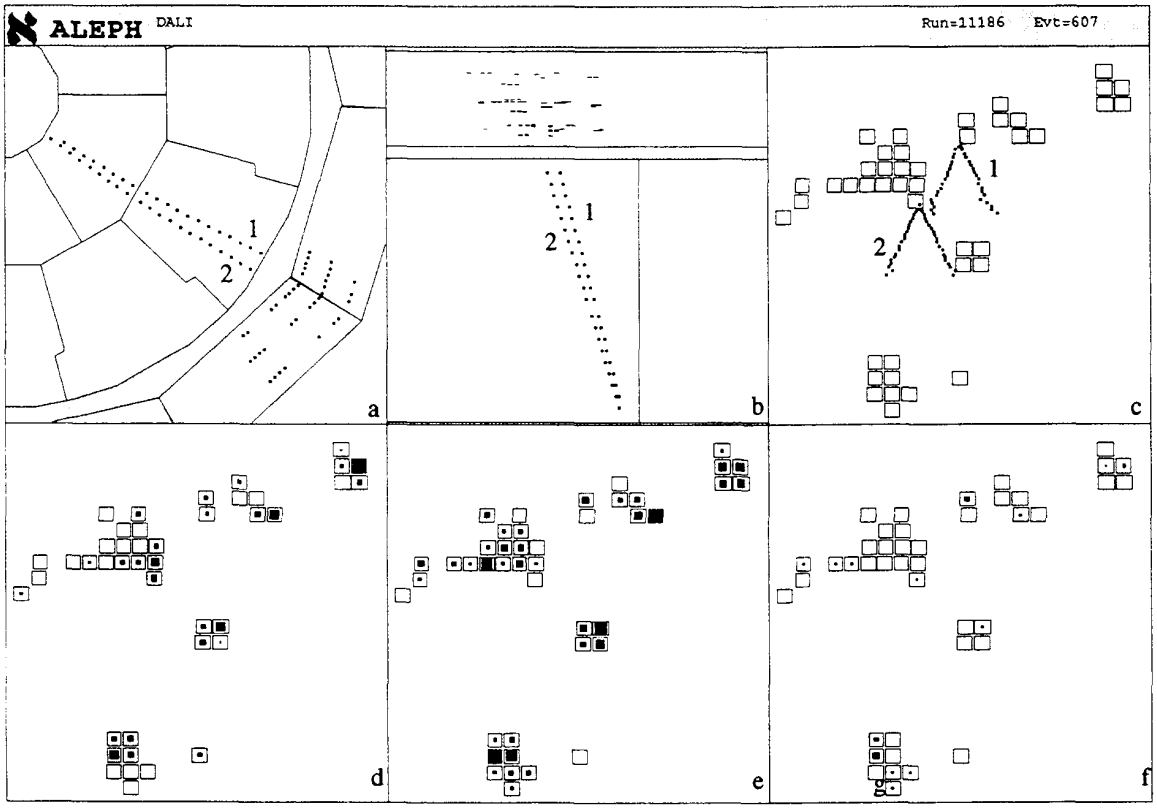

Fig. 13:Association of TPC tracks to a calorimeter

a) Y/X b) ρ'/Z c) V-Plot + calorimeter islands

d) φ / ϑ of calorimeter layer 1 e) φ / ϑ of calorimeter layer 2 f) φ / ϑ of calorimeter layer 3

The area of the squares is proportional to the deposited energy.

5.5. The V-Plot for super high multiplicity events

Figure 14 shows the front view, *Y/X*, for a simulated "super event" with 221 tracks. The simulation was accomplished by superimposing many events from the ALEPH TPC. Only few tracks can be identified in the front view even when blown up (see figure 14b). The display of such "super events" in other conventional projections yields even more difficult pictures due to cycloidal track patterns. The simultaneous use of two conventional 2D projections, in order to examine the tracks from several sides, excludes itself, as it is practically impossible to correlate the tracks. These projections can only be used, if one succeeds to apply cuts so that sufficiently few tracks are displayed.

Track identification is possible via the V-Plot (figure 15a), as long as the tracks leave the chamber, i.e. do not spiral. By blowing up crowded regions (the framed region in 15a is blown up in 15b) practically all non spiraling tracks can be identified.

By defining a volume through an angular section, as discussed in chapter 5.3, single tracks or groups of tracks can be selected and displayed in conventional projections. The hits contained in the rectangle of figure 15b are shown in *Y/X* in figure 15c, where tracks are easily recognized. This track selection acts like a depth cut (ϑ-cut, not Z-cut!) on *Y/X*. Despite the high multiplicity of such events it may be possible to generate conventional pictures suitable for talks and papers by applying selections of this type.

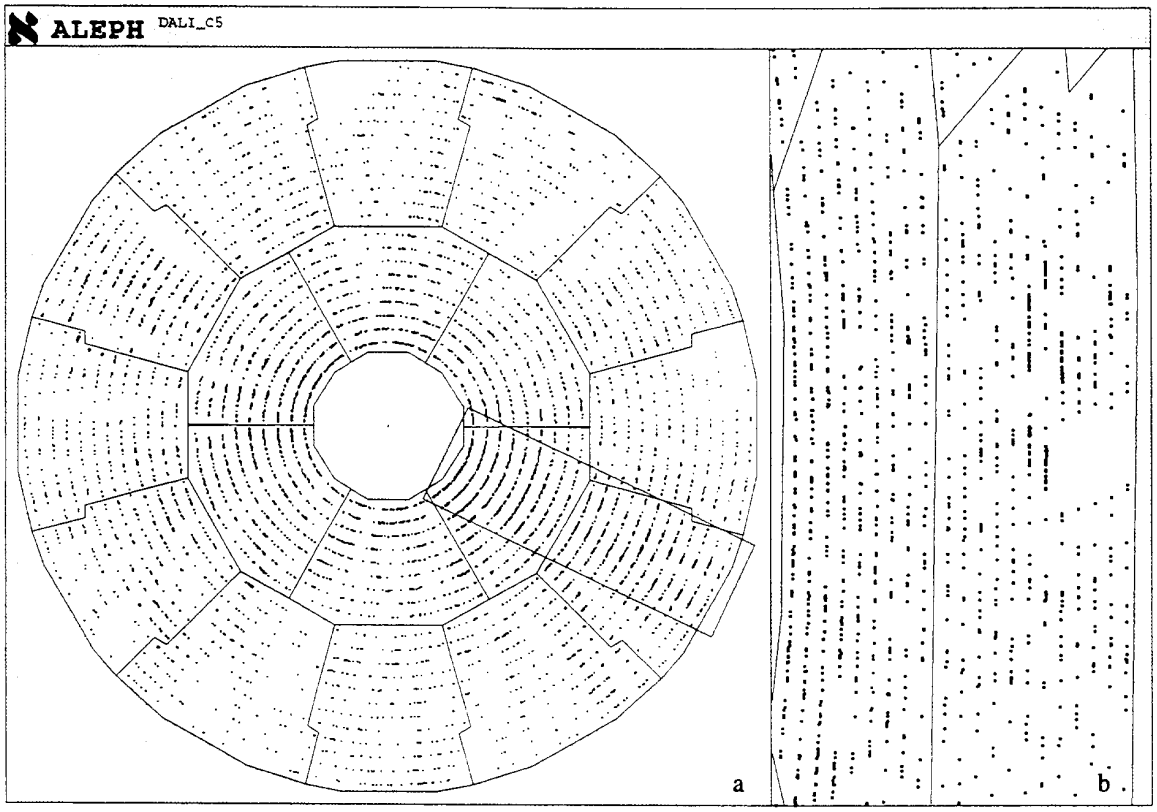

Fig.14: Super high multiplicity event with 210 tracks
a) Y/X b) blow-up of Y/X defined by the rectangle in figure a

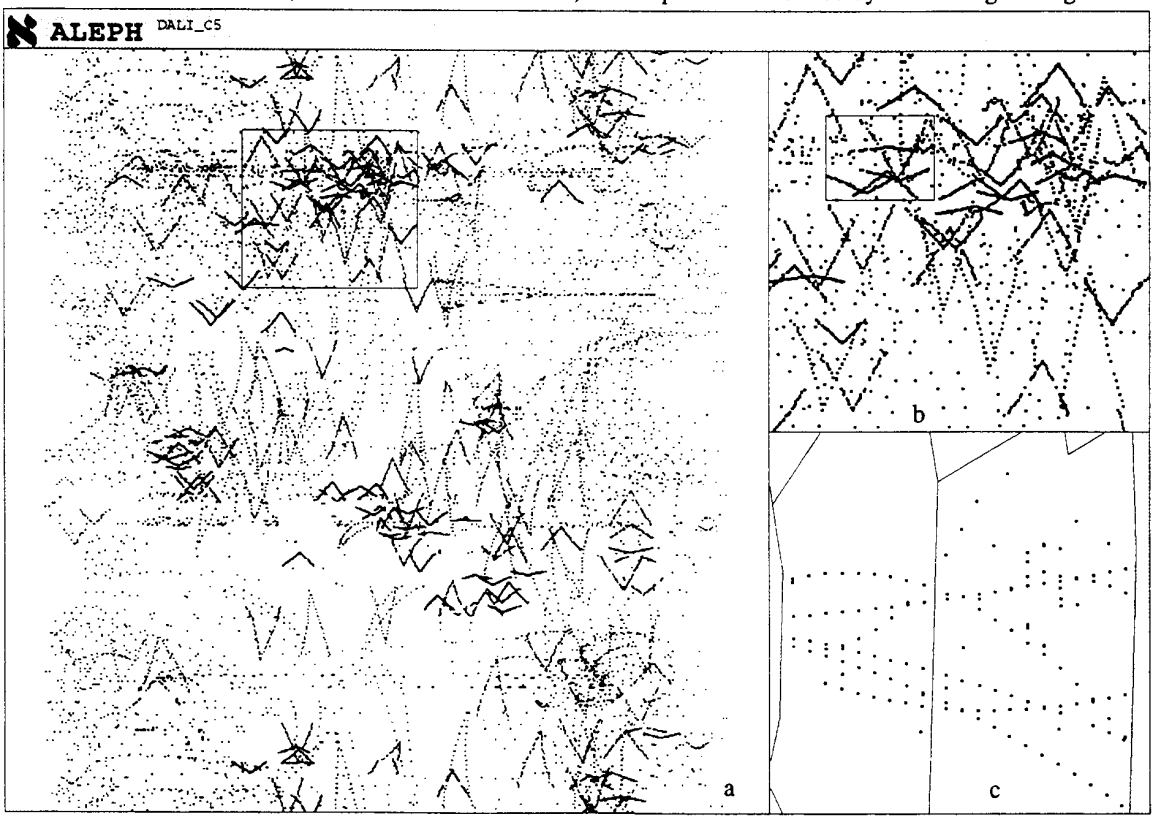

Fig.15: Super high multiplicity event with 210 tracks
a) V-Plot b) blow-up of the V-Plot c) Y/X of the hits selected through the rectangle of figure b.

5.6. Generalisation of the V-Plot

The V-Plot technique is constrained to 3D data only, which might either consist of 3D hits or of 3D track segments. In the latter case the spatial position may be measured directly or may be determined through the averaging of sets of hits or may be obtained through other methods.

From the special form of the V-Plot, described above, we will try to deduce general rules to construct a V-Plot, namely:

- The V-Plot is a superposition of two symmetric projections. For each 3D hit two points are drawn. The position of the center between them and their distance kD are calculated from the coordinates of the hits. The angle β under which the two points are drawn can be chosen in a convenient way. It is important that no other information than the 3D position of the hit is used. Especially, the association of a hit to a track is not taken into account.
- The projections must be chosen in a way to (approximately) linearize tracks and to compress all of them simultaneously. An optimal compression is achieved, if for $k=0$ a radial straight track is seen as a single point.
- The distance kD between the two point images is a measure for the distance R of the 3D hit from the center.
- H,V and D should be chosen in such a way that charge and momentum can be estimated.

If a variable U (or a function of variables) is (approximately) constant for all points of a track, then H,V,D and β may subsequently be modified through this variable in order to fulfill the above requirements and to yield a usable picture, e.g. H is changed to $H'=HF(U)$. Under this transformation straight V-arms remain straight.

Various realizations of V-Plots are published elsewhere [5]. In the next chapter one of them is presented.

5.7. The V-Plot for straight track sections outside a magnetic field (TPC Tracks of the NA35 Experiment)

In the fixed-target heavy-ion experiment - NA35 - at the SPS/CERN a large number of particles leaves the target in very forward direction, defined as X-direction [6]. A perpendicular homogeneous magnetic field (in Z-direction) bends the particle trajectories in the X-Y plane. About six meters downstream, outside the magnetic field, straight track segments are recorded by a TPC, delivering 3D track hits. Figure 16a shows the setup in Y/X, with the vertex at the very left and a rectangular block of the TPC hits at the right. A blowup of the hits is shown in figure 16d and the other two projections Y/Z and Z/X in figures 16b,c respectively. The only projection, where tracks can be distinguished, is Y/Z. However, it is difficult, if not impossible, to estimate charge and momentum.

The straight tracks in the TPC can be described by $Y = aX + b$ and $Z = cX$, where the gradient a depends on the direction and the momentum of the track; the offset b is an approximate measure of the track momentum, hence is of higher interest.

The general V-Plot rules of the previous chapter are fulfilled by setting

$H = \frac{Z}{X}$, $V = \frac{Y}{X}$, $D = X_1 X_2 (\frac{1}{X_1} - \frac{1}{X}) \approx X - X_1$, where X_1 and X_2 define the position of the entry and the exit plane of the TPC, respectively. Then one displays V versus $H \pm kD$.

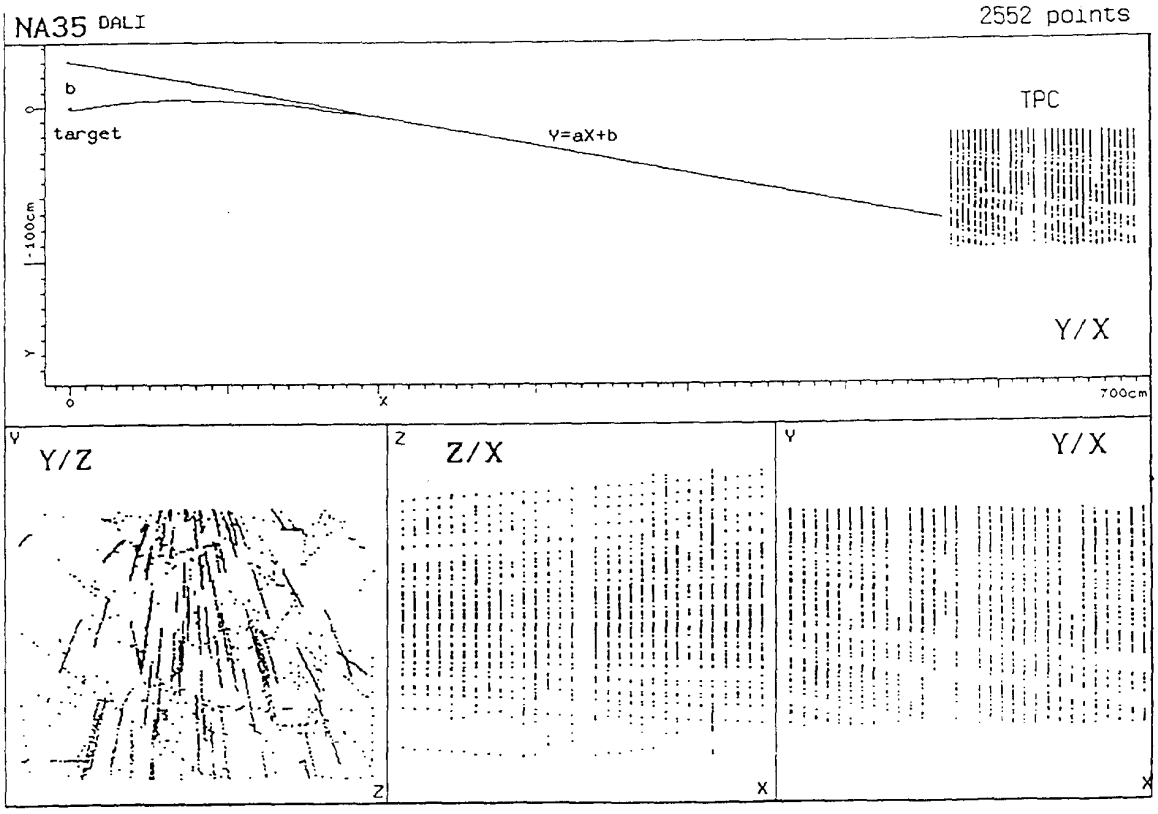

Fig. 16: An event from the NA35 TPC
a: setup of the experiment in Y/X
b) Y/Z c) Z/X d) Y/X

If $k=0$, this V-Plot is identical to $\frac{Y}{X} / \frac{Z}{X}$, which is rather similar to the best of the above projections, namely Y/Z (figure 16b); the interpretation of the V-position is therefore straightforward. In $\frac{Y}{X} / \frac{Z}{X}$ the image of a radial straight tracks ($b = 0$) is reduced to one point. The V-arms are drawn in the symmetric projections $V/(H+kD/2)$ and $V/(H-kD/2)$. For the points of a single track ($\frac{Z}{X} = c$) these projections are identical to $\frac{Y}{X}$ / $\frac{1}{X}$ apart from a linear transformation. As discussed already in chapter 3.5, straight tracks transform into straight tracks in this projection, as $\frac{Y}{X} = a + b\frac{1}{X}$. Therefore the arms of the V are straight, their gradient b is a measure of the particle momentum and the V-direction gives its charge, so that one gets the same features as for the V-Plot of the ALEPH TPC. One feature is especially important, namely that both, momentum and charge, can be estimated locally from the display of the TPC hits only without displaying the vertex point.

Figure 17 shows a simulation of track hits with either 2, 6 or 12 GeV/c in Y/Z and as V-Plot. It is evident, that the shape of the track images, the V's, depends only on momentum and not on the position of the tracks.

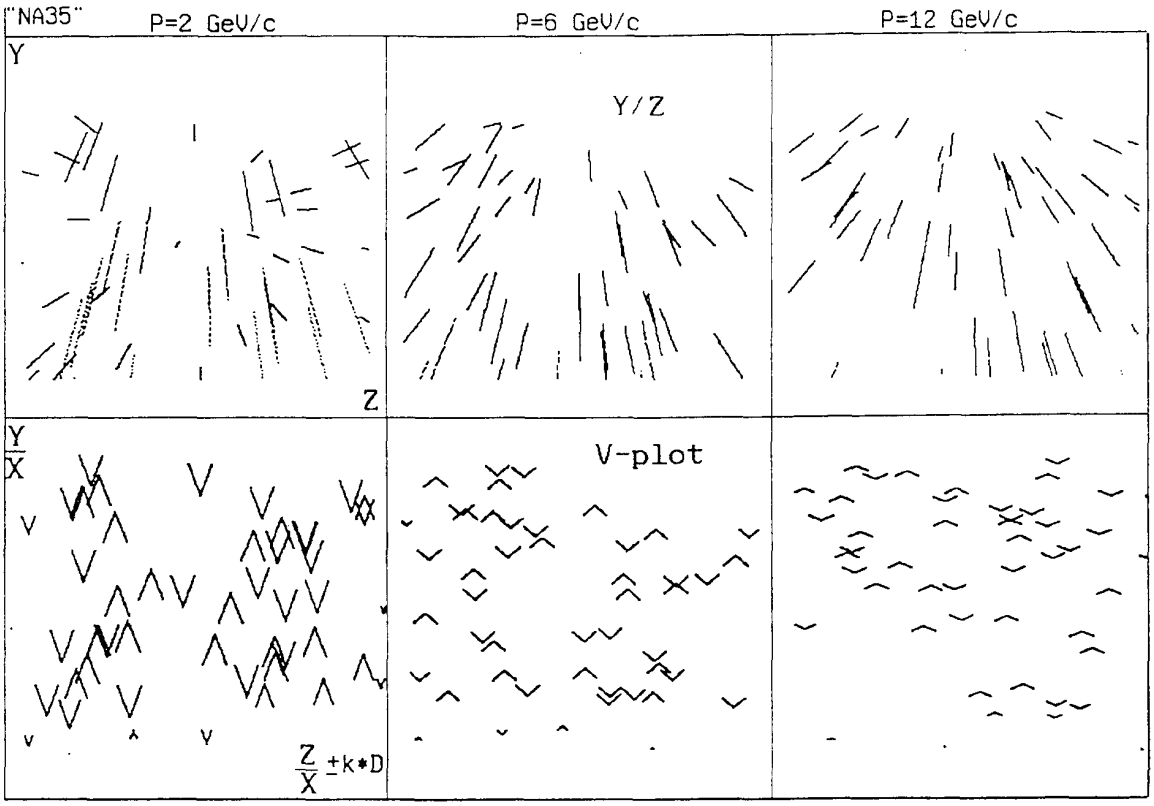

Fig. 17:Simulated hits of tracks with predefined momenta P (without measuring errors)

a) P = 2 GeV/c , *Y / Z* b) P = 6 GeV/c , *Y / Z* c) P = 12 GeV/c , *Y / Z*

d) P = 2 GeV/c , V-Plot e) P = 6 GeV/c , V-Plot f) P = 12 GeV/c , V-Plot

The NA35 event shown before in figure 16 is displayed in figure 18 as a V-Plot, on which the tracks are easily identified, and from which one can extract momentum and charge of the particles[1].

6. The Puzzle-Plot, a Three Dimensional Representation of Calorimeter data

Figures 13d,e,f show three layers of a calorimeter side by side, so that one can follow the shower development by comparing the three pictures, as discussed before. It is possible to recognize, which cells in the different layers form a cluster, i.e. belong to the same shower. Thereby it is possible to verify independently the clustering algorithm of the pattern recognition program. With increasing number of layers, however, this gets more and more tedious.

1. The data originate from one of the very first events ever recorded in the NA35 TPC, which was not yet well aligned.

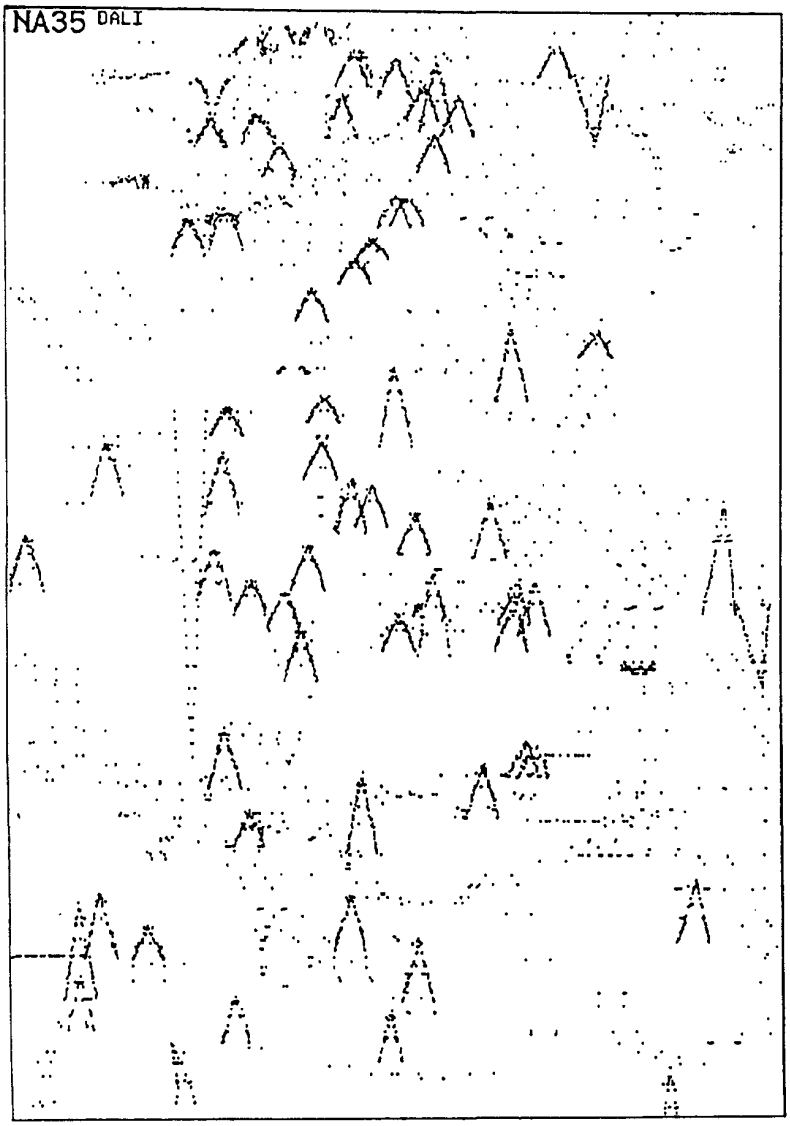

Fig. 18: V-Plot of the same NA35 event as in figure 16

An example of a calorimeter with a large number of layers is the ALEPH Silicon Calorimeter, SICAL. It has a cylindrical structure and consists of two parts 2.5 m down and up stream from the center with a length of 12 cm, an inner radius of 6 cm and an outer one of 14.5 cm. Each cylinder is divided into 12 disks, each disk is divided into 16 rings and each ring into 32 angular sections with $\Delta\varphi = 360^{o} / 32 = 11.25^{o}$. Thus the detector consists of 6144 cells in 12 axial and 16 radial layers. Each of the disks is rotated by $\Delta\varphi/3$ as compared to the previous one, i.e. the disks are "staggered".

In color plate 12a all active cells are displayed in the wire frame technique in a perspective view. A section is blown up in color plate 12b. All blue cells are considered by the clustering algorithm to belong to the same cluster. The same is true for the pink cells. The yellow cells do not touch these two clusters and have too little energy to form a cluster themselves, i.e. they are regarded as noise by the clustering algorithm.

However, the picture is very complicated due to the large number of active cells and due to the fact, that perspective drawings are less well comprehensible if lines are curved and the objects have different orientations. The picture would get even more complicated if in addition one would try to display the amount of energy deposited in the active cells.

By use of such pictures it is possible to prove, that clusters do not touch each other, if at least one suitable viewing direction can be found, where they appear separated (see the blue and pink clusters in color plate 12). It is more tedious to prove that all noise cells (yellow) are not connected to one of the clusters, as it may be necessary to select a different direction of view in each case. For the usual complex clusters, however, it is impossible to identify visually all cells belonging together. The Puzzle-Plot, explained below, offers a way out. However, it is not intuitively understandable.

The rules to interpret the Puzzle Plot are best explained by ignoring for a moment, what is known about the calorimeter. Color plate 13a shows a Puzzle Plot and 13b the blowup of a section. The blowup shows 10 black fields separated by white lines, where each field contains one or several "triple-crosses". A triple cross is composed of one vertical bar and three equidistant horizontal bars of identical color. The crossing points of the bars lie along three diagonal lines and are emphasized by a black spacing between the bars. The yellow one in 13b may serve as example.

Next we try to find all connected triple crosses applying the following rules:

Triple-crosses in neighboring fields are connected if:

- 1) one (or two) of their horizontal bars touch each other, or
- 2) their vertical bars touch each other.

Triple-crosses in the same field are connected, if:

- 3) their vertical and horizontal bars have minimum distance between each other, which in this example is equal to the distance of the pink bars in one field.

One sees clearly, that all blue triple-crosses in 13b are connected directly or indirectly via other triple crosses. The same is true for the pink ones, whereas the yellow one is unconnected.

There is a close correspondence between these rules and the problem to find clusters in the SICAL, as the black fields are a mapping of the towers arranged vertical to the Z-axis and the triple crosses describe the position of the active calorimeter cells. The position of a triple-cross is defined by three independent variables. Two *(H,V)* define the position of the field in which it is drawn, and one *(D)* defines the position of the triple-cross inside the field along the diagonal lines. The position of a cell in the SICAL is defined by φ, Z and ρ. If one sets $V = \varphi$, $H = Z$ and $D = \rho$, the calorimeter is mapped onto the Puzzle-Plot, so that it is possible to visualize the cells in all three dimensions. This allows to check the association of cells to clusters.

The arrangements of the fields reflects the staggering, which necessitates the use of three horizontal bars in order to visualize the connection in Z-direction (rule 1 above).

One notices from color plate 13a, that in the fields denoted by a ' * ', triple crosses exist, which cannot be connected to the blue cluster, directly or indirectly. This is due to the fact, that the real clustering algorithm of the ALEPH SICAL allows the connection of cells, if they touch at a border lines parallel to the Z-axis, i.e. triple crosses in neighboring fields above or below are connected if:

- 4) their vertical lines are displaced by one step.

The application of this rule is easy in the puzzle plot very difficult in the wire frame representation.

The special form of the Puzzle-Plot as described above may of course vary depending on the structure of the calorimeter to be displayed. The triple-crosses can be regarded as symbols displaying the depth of the cell. There may be other symbols useful for this purpose.

The representation of the SICAL data via the Puzzle-Plot allows in a simple way to represent in addition the energy deposit in the active cells. At the center of the three horizontal lines of a triple-cross a horizontal line of a different color (red and white in our example) is drawn, the length of which is proportional to the deposited energy. Thus one gets the visualization of a three dimensional scalar field.

7. Conclusions

Visual representations are used for two different purposes, namely for

- presentations, i.e.talks and papers,
- visual analysis.

If pictures are used in presentations they should be intuitively understandable, without requiring long explanations. If a picture is not just used for eye catching, the information the lecturer or writer wants to pass to his audience must be clear from the picture. This is even more demanding, if a picture is shown in a talk for a short time only. To this aim pictures must be sufficiently simple, still matching the complexity of detectors and events.

In the case of a cylindrical detector the best pictures are obtained using cross-sections, i.e.:

- ρ'/Z as side view and Y/X as front view, with the endcaps omitted in Y/X. If these projections are applied, the various subdetectors do not overlap, so that both hits and subdetectors can be drawn together and hits fall onto the image of the subdetector, by which they were recorded.

These images can be further improved by:

- applying a (non linear) fish eye transformation of the front view, so that the inner chambers are enlarged and the outer ones reduced in size;
- displaying the energies deposited in the calorimeters as histograms in the form of structured areas;
- coloring the subdetectors;
- choosing suitable colors for hits and tracks. Tracks are better separated, if close ones are colored differently.

Three dimensional information can be transmitted by

- showing Y/X and ρ'/Z side by side. In this case color may be used to correlate objects in the different pictures.

These methods yield clear pictures in the case of experimental setups as the ALEPH detector. Furthermore, it is of big help to carefully select events, which show the required features, but which also give good pictures.

However, if events with much higher multiplicities are to be shown, a display of the data may yield useless pictures, i.e. the limits of these methods may be met. A way out might be the application of one of the following methods, namely

- to draw the data in a simpler form, i.e. tracks (lines) instead of hits (points),
- to restrict the amount of displayed data by use of information given by the pattern recognition program, e.g. by a cut on track momentum,
- to display data from sufficiently small volumes, where the problem of how to find and define such a volume arises,
- to use non-conventional projections like the V-Plot or the Puzzle Plot, which yield clearer pictures. However, they have the big disadvantage, that the listener or the reader is required to have the necessary knowledge for their interpretation.

The above conclusions are also valid for the visual analysis of tracks, where it is often necessary to display the basic data, i.e. display the hits instead of tracks. It is normally not possible to restrict the analysis to specially selected, clear events.

Most events have a large amount of tracking information. The track recognition is drastically improved through the following concepts:

- Track compression, i.e. a low magnification in track direction and a large one perpendicular to it.
- Track linearisation, which facilitates compression, but also recognition and visual extrapolation of the tracks. In the case of helices this is achieved using angular projections.
- Use of projections which allow the local estimation of track features, i.e. particle charge and momentum.

Through the first two methods it is possible to increase the magnification of a track in its full length to a level, where the errors of data recording become apparent, i.e. the limits imposed by screen and eye resolution are overcome.

If three dimensional data are available, two further concepts get important, namely

- the use of orthogonal projections,
- the overlay of two projections to transfer 3D information.

A good realization of the above concepts is found in the V-Plot, the mathematical formulation of which depends on the experimental setup. Furthermore, the V-Plot is a powerful means to extrapolate tracks to calorimeter representations like the Lego Plot.

Whereas the limits of the conventional methods seem to be reached when examining difficult events, the limits of the V-Plot technique still seem to be further away. This technique is however constrained to real three dimensional data, i.e. 3D hits and 3D track segments.

Calorimeter data are best displayed as Lego Plot or through pictures with similar structure, e.g. φ/ϑ, but different energy representation. Different layers projected side by side allow to judge the shower development, where the island representation helps to associate the clusters in different layers.

The use of this technique, however, gets very tedious, with increasing granularity of the calorimeter, i.e. if many layers exist. A way out is shown in the Puzzle Plot, although it may be limited due to screen and eye resolution. It should be tried to modify its principles, if large

showers covering very many cells, i.e. large volumes, are to be displayed.

In short, the purpose of visual representations, namely to transfer data from the computer to the human brain, can still be accomplished in a fast, unambiguous and efficient way. Even for complex detectors and events, display methods are available to present the full data. There seem to exist more powerful concepts for the display of 3D data than for 2D data. However, the price to be paid is the use of more abstract representations. If one is ready to accept this complication, visualization of events will continue to serve as a helpful tool for presentation and analysis.

8. Acknowledgements

The successful construction and running of the ALEPH detector by the collaboration provided the events, for which the methods described in this paper were developed. During development of these techniques we have had input from many of our colleagues in ALEPH. We owe special thanks to Chris Grab, Salvador Orteu, Mark Parsons, Raimund Vogl and Rongfen Xu for their valuable contributions to the program and to Brigitte Bloch-Devaux, Jürgen Knobloch, Dieter Schlatter and Jack Steinberger for helpful discussions and suggestions. For information on NA35 we thank Ingo Schneider and the NA35 collaboration for providing us with data. This paper was written with the program FrameMaker. We acknowledge gratefully Joe Boudreau, Robert Cailliau and Mick Storr for their expert assistance.

9. References

[1] D.Decamp et al., Nucl.Instr.Meth. A294 (1990) 121.

[2] H.Drevermann and W.Krischer, Nucl.Instr.Meth. A239 (1985) 160.

[3] This method was proposed by M.Mermikides

[4] Rainer Wolf und Dorothea Wolf:
Vom Sehen zum Wahrnehmen: Aus Illusionen entsteht ein Bild der Wirklichkeit
VCH Verlagsgesellschaft mbh : *Vom Reiz der Sinne*
edited by Alfred Maelicke, ISBN 3-527-28058-8

[5] H.Drevermann, C.Grab and B.S.Nilsson,
How to Represent Three Dimensional Data of Events from High Energy Physics?
Proceedings of the international conference on Computing in High Energy Physics 91,Tsukuba, Japan, page 545. Universal Academy Press, INC.-Tokyo

[6] J.W.Harris et al., Nucl.Instr.Meth. A315 (1992) 33.

Further Reading:

H.Drevermann and C.Grab, Int. Jour. Mod. Phys. C1 (1990) 147.

H.Drevermann, C.Grab, D.Kuhn, B.S.Nilsson and R.K.Vogl:
A New Concept for Visual Analysis of Three Dimensional Tracks
John Wiley & Sons: *New Trends in Animation and Visualization*
edited by N.Magnenat Thalmann and D.Thalmann